PLOS ONE

RESEARCH ARTICLE

USP5 enhances SGTA mediated protein quality control

Jake Hill[1,2], **Yvonne Nyathi**[1,2]*

1 School of Life Sciences, Joseph Banks Laboratories, University of Lincoln, Lincoln, United Kingdom, **2** School of Chemistry and Bioscience, Faculty of Life Sciences, University of Bradford, Bradford, United Kingdom

* y.nyathi@bradford.ac.uk

OPEN ACCESS

Citation: Hill J, Nyathi Y (2022) USP5 enhances SGTA mediated protein quality control. PLoS ONE 17(7): e0257786. https://doi.org/10.1371/journal.pone.0257786

Editor: Jeffrey L. Brodsky, University of Pittsburgh, UNITED STATES

Received: September 9, 2021

Accepted: July 11, 2022

Published: July 27, 2022

Data Availability Statement: All relevant data are within the paper and its Supporting Information files.

Funding: The author(s) received no specific funding for this work.

Competing interests: The authors have declared that no competing interests exist.

Abstract

Mislocalised membrane proteins (MLPs) present a risk to the cell due to exposed hydrophobic amino acids which cause MLPs to aggregate. Previous studies identified SGTA as a key component of the machinery that regulates the quality control of MLPs. Overexpression of SGTA promotes deubiqutination of MLPs resulting in their accumulation in cytosolic inclusions, suggesting SGTA acts in collaboration with deubiquitinating enzymes (DUBs) to exert these effects. However, the DUBs that play a role in this process have not been identified. In this study we have identified the ubiquitin specific peptidase 5 (USP5) as a DUB important in regulating the quality control of MLPs. We show that USP5 is in complex with SGTA, and this association is increased in the presence of an MLP. Overexpression of SGTA results in an increase in steady-state levels of MLPs suggesting a delay in proteasomal degradation of substrates. However, our results show that this effect is strongly dependent on the presence of USP5. We find that in the absence of USP5, the ability of SGTA to increase the steady state levels of MLPs is compromised. Moreover, knockdown of USP5 results in a reduction in the steady state levels of MLPs, while overexpression of USP5 increases the steady state levels. Our findings suggest that the interaction of SGTA with USP5 enables specific MLPs to escape proteasomal degradation allowing selective modulation of MLP quality control. These findings progress our understanding of aggregate formation, a hallmark in a range of neurodegenerative diseases and type II diabetes, as well as physiological processes of aggregate clearance.

Introduction

Newly synthesised membrane proteins are triaged between biosynthetic pathways targeting them to subcellular compartments such as the mitochondria and the endoplasmic reticulum (ER) and degradative pathways operating in the cytosol [1]. Timely degradation of membrane proteins that mislocalise to the cytosol is necessary to prevent their accumulation and aggregation which is linked to a range of pathologies [2, 3]. Therefore, a variety of intricate protein quality control mechanisms are dedicated to eliminating these mislocalised membrane proteins (MLPs) and maintaining protein homeostasis in mammalian cells [4]. Another layer of

protein quality control for membrane proteins occurs at the ER membrane. Misfolded membrane proteins that are delivered to the ER and fail to integrate into the ER membrane are targeted for ubiquitination and subsequent degradation via the endoplasmic-reticulum-associated protein degradation pathway (ERAD) [5, 6]. These quality control mechanisms collectively act to ensure that mislocalised or misfolded membrane proteins are degraded at any stage during their targeting and integration into the ER membrane [7].

The fate of MLPs that expose hydrophobic amino acids in the cytosol is decided via a delicate collaboration between factors that promote ubiquitination and those that promote deubiquitination of the MLPs [8, 9]. Ubiquitination occurs via the action of an array of enzymes; an E1 ubiquitin activating enzyme, an E2 ubiquitin- conjugating enzyme and an E3 ubiquitin ligase, acting in sequence to polyubiquitinate the substrate for subsequent proteasomal degradation [10]. Ubiquitination is a highly dynamic and reversible process due to the action of deubiquitinating enzymes (DUBs) which act as ubiquitin proteases, thereby antagonising the action of the E3 ligases and preventing the proteasomal degradation of substrates [11, 12].

It has long been known that DUBs are important for generating a pool of free ubiquitin in the cell [13, 14]. However, recent evidence suggests a role for DUBs in the regulation of many cellular processes by fine-tuning or modulating substrate ubiquitination and degradation [14]. A typical example is the DUB Ataxin-3, which acts to limit the length of ubiquitin chains built on substrates by CHIP (C-terminus of Hsc70 Interacting Protein) a mammalian E3 ligase involved in cytosolic protein quality control [15] In addition, some cytosolic localised DUBs are important in kinetic proofreading and discrimination of membrane proteins that should be degraded by the proteasome [16] While DUBs localised on the proteasome, such as UCHL5 and USP14 can delay the degradation of proteasomal substrates [17] Moreover, DUBs are now known to have an important role in ubiquitin chain editing by selectively trimming either K48 ubiquitin conjugates or K63 linked ubiquitin chains on substrates to regulate degradation by the proteasome or via autophagy, respectively [18, 19].

Recent studies suggest a role for USP13 in ERAD [20, 21], and USP20/33 in deubiquitinating tail anchored membrane proteins prior to their insertion into the ER membrane [22]. Although such details about the role of specific DUBs in membrane protein quality control is beginning to emerge, this knowledge in still in its infancy. This is in stark contrast to the tremendous progress that has been made towards our understanding of the E3 ligases that play a role in membrane protein quality control. In yeast the cytosolic ubiquitin ligases Ubr1p [23], San1P [24] and the ER resident Doa10p and Hrd1p ubiquitinate substrates for proteasomal degradation [25, 26]. The mammalian orthologues of Hrd1p (HRD1) [27], Hrd1p homologue gp78 [28] and Doa10p (MARCH6) [29] are known to promote ERAD. Moreover, the ligases MARCH6 and TRC8 were also shown to promote the ubiquitination of tail anchored proteins at the cytosolic face of the ER [30], while RNF126 was shown to promote ubiquitination of MLPs [31].

Several studies have also demonstrated a role for the ubiquitin proteasome system in the degradation of MLPs [4, 9, 31–35]. Among the factors known to be involved in regulating this degradation is the BCL2-associated athanogene 6 (BAG6) [1, 36, 37], the cochaperone SGTA (small glutamine-rich tetratricopeptide repeat protein alpha) [1, 9, 32] and a host of their diverse interacting partners. SGTA, is a homodimer, with an N-terminal domain which interacts with UBL4A (the ubiquitin-like protein 4A), and BAG6 [38, 39], a central TPR domain which interacts with Hsp70 and Hsp90 chaperones [40, 41], and a C-terminal domain capable of binding hydrophobic substrates [42].

A BAG6/SGTA quality control cycle dictating the fate of MLPs is proposed to be operating at the proteasome [43]. In this cycle, BAG6 recruits RNF126, an E3 ubiquitin ligase which catalyses the selective ubiquitination of MLPs for subsequent degradation by the proteasome

[31, 44]. On the other hand, SGTA promotes deubiquitination thereby giving substrates a chance to escape proteasomal degradation [9, 32]. Therefore, in the context of the BAG6/SGTA cycle, it is plausible that an interaction of SGTA with deubiquitinating enzymes could provide SGTA-bound MLPs access to the enzyme(s) which mediate deubiquitination, thereby delaying the clearance of the MLPs and perhaps favour their targeting to the ER and subsequent membrane integration [43]. However, the deubiquitinating enzyme(s) that play a role in this process have not been defined to date. In this study we employed pull downs and mass spectrometry to identify DUBs that interact with SGTA. We show that USP5 is in complex with SGTA using co-immunoprecipitation, and that this interaction is necessary for the ability of SGTA to increase the steady state levels of MLPs. The implications of this study to our understanding of mislocalised membrane protein quality control is discussed.

Materials and methods

All cell culture and standard reagents were purchased from Fisher Scientific (Loughborough, UK). Antibodies to opsin and V5 were previously described [32]. Commercially available antibodies against the following targets were purchased from the indicated suppliers, tubulin and GFP were purchased from Abcam (Cambridge, UK), USP9X (#A301-350A), USP5 (#A301-542A), USP14 (#A300-920A) and USP10 (#A300-900A) antibodies were purchased from Bethyl Laboratories Inc. (Montgomery, USA). Bortezomib was purchased from Selleckchem (Munich, Germany), Leupeptin and Pepstatin A were purchased from BIOMOL (Hamburg, Germany).

Plasmids

Plasmids for the overexpression of SGTA-V5 and Pex19-V5 were previously described [43]. Ub-M–GFP (#11938) and Ub-R–GFP (#11939) plasmids described in [45] were purchased from Addgene. HA tagged USP5 (#22590) was purchased from Addgene and subcloned into pcDNA5 mammalian expression vector. The plasmid for the expression and USP5^{C335A} mutant was created by site directed mutagenesis using the HA tagged USP5 as template and primers carrying the mutated codons. DNA sequencing was used to verify the mutant prior to use. The 3x NNP/AAA (NNP positions at 226–228, 239–241 and 255–257) variant of SGTA-V5 was previously described [46].

The pET28-TxA-SGTA wild type plasmid for the expression and purification of WT SGTA was previously described [46]. This plasmid was generated by cloning WT SGTA into BamHI/XhoI restriction sites of a pET28c vector modified to encode an N-terminal thioredoxin A (TxA) fusion protein followed by a hexa-histidine tag. Plasmids for the expression and purification of SGTA_TPR double mutant (SGTA$^{K160E/R164E}$) and SGTA_UBL double mutant (SGTA$^{D27R/E30R}$) mutant were created by site directed mutagenesis using pET28-TxA-SGTA wild type plasmid as template and primers carrying the mutated codons. DNA sequencing was used to verify the mutants prior to use.

Cell culture

The inducible stable HeLa Flp-In T-REx cell lines expressing OP91 or opsin degron (OpD) were previously described in [32, 47], respectively. The HeLa cells were maintained in DMEM containing 10% fetal bovine serum and 2 mM L-glutamine at 37˚C under 5% CO2. At alternate passages, DMEM was supplemented with 100 μg/ml hygromycin B and 4 μg/ml blasticidin S. Transfections of plasmid DNA were performed using Lipofectamine 2000 (Life Technologies, Carlsbad, CA, USA) in accordance with the manufacturer's instructions. 6 hours post-transfection, OP91 or OpD expression was induced by treating the cells with

DMEM containing 1 μg/ml tetracycline followed by growth for an additional 16–18 hours. Where indicated, 10 nM bortezomib or 100 μM leupeptin and 1 μg/ml pepstatin were added to cells 20 hours prior to analysis.

Knockdown experiments

For siRNA experiments, 20 nM of siRNAi duplexes (from Dharmacon (Chicago, IL, USA), were transfected into cells using INTERFERin (Polyplus, Illkirch, France) according to the manufacturer's instructions. 48 hours post-transfection the cells were transiently transfected with the appropriate DNA constructs (where necessary) and harvested after a further 24-hour incubation. Non-targeting control duplex [Cat# D-001810-01-20] and synthetic siRNA duplexes, USP5 siRNA1; [Cat#: D-006095-02-0002] and USP5 siRNA2; [Cat# D-006095-03-0002] targeting the USP5 gene [13], and the USP9x ON-TARGETplus siRNA [Cat# J-006099-06-0002] were purchased from Dharmacon (Chicago, IL, USA). SiRNA target sequences for SGTA and USP14 were 5′-ACAAGAAGCGCCUGGCCTATT-3′ [48] and 5′- AGAAA TGCCTTGTATATCATT-3′ [49] respectively. Depletion of Bag6 and RNF126 was achieved by using the siRNA duplexes 5′-UUUCUCCAAGAGCAGUUUATT-3′ and 5′-CAUCCCGGACGGU ACUUCUGCCACU-3′, respectively.

Real-time RT-PCR

To quantify OP91 expression levels, total cellular RNAs were isolated using TRIzol™ Plus RNA Purification Kit (Invitrogen, Carlsbad, CA) and used for first-strand cDNA using the Sensi-FAST™ cDNA Synthesis (Bioline, Memphis, TN, USA). Quantitation of the OP91 transcript was done by quantitative PCR using the SensiFAST SYBR® Hi-ROX Kit (Bioline, Memphis, TN, USA) and the StepOnePlus™ Real-Time PCR detection system (Applied biosystems by Thermo Fisher Scientific). The expression of GAPDH was used as the internal control. For the primers 5 pmol of OP91 AGGGCCCAAACTTCTACGTG (forward) and AGCGTGAGGAAGTTG ATGGG (reverse) and GAPDH, GAAGGTGAAGGTCGGAGTC (forward) and GAAGATGGTGA TGGGATTTC (reverse) were used. PCR conditions were 50˚C for 2 min, 95˚C for 10 min, and then 40 cycles of 95˚C for 15 s and 60˚C for 1 min. Melt curve analysis was performed to verify the specificity of the reaction and cycle threshold values (Ct values) were used to calculate the -fold differences using the comparative Ct (ΔΔCt) method.

Protein purification

Plasmids for protein expression were transfected into *E. coli* BL21 (DE3) strains and protein expression was induced by using 0.5 mM isopropyl-β-D-thiogalactopyranoside (IPTG) at OD600 ≈ 0.8, followed by overnight incubation at 22˚C. Cells were harvested and resuspended in lysis buffer (20 mM potassium phosphate, pH 8.0, 300 mM NaCl, 10 mM Imidazole, 50 mM Tris-HCl, 10% glycerol, supplemented with protease inhibitors -EDTA (Roche, Burgess Hill, UK), and 1 mM PMSF and lysed by sonication. Cell debris was removed by centrifugation, and the soluble fractions were purified using nickel affinity chromatography (Qiagen, Manchester, UK) and eluted with lysis buffer containing 300 mM imidazole, followed by dialysis into phosphate buffered saline pH 7.4. Gel filtration was carried out using a HiLoad 16/60 Superdex 200 column (GE Healthcare, Amersham, UK), previously equilibrated in buffer containing 10 mM potassium phosphate pH 6.0, 100 mM NaCl and 50 mM Tris-HCl. Proteins were concentrated using Vivaspin concentrators (Sartorius Stedin) and the sample purity and homogeneity was assessed by SDS-PAGE.

Coupling of purified recombinant protein to resin

UltraLink Biosupport resin (Thermo Scientific, Pierce) were incubated with coupling buffer (0.6M Sodium Citrate, 0.1M MOPS, pH 7.5) and equimolar amounts of recombinant protein WT SGTA, SGTA mutants ($SGTA^{K160E/R164E}$ and $SGTAD^{27R/E30R}$) or Thioredoxin, overnight at 4˚C, to allow covalent coupling via primary amines. 3M ethanolamine pH 9.0 was used to quench the reaction after coupling. Beads with coupled recombinant proteins were washed for 15 minutes with PBS and 1M NaCl in turn. Beads were further washed 3 times in PBS and re-suspended in PBS for storage at 4˚C.

Pull-down assays

Beads coupled to recombinant WT SGTA, SGTA mutants ($SGTA^{K160E/R164E}$ and $SGTA^{D27R/E30R}$) or Thioredoxin were incubated with rabbit reticulocyte lysate or HeLa lysate overnight. Resins were washed three times in buffer containing 40mM HEPES-KOH, pH 7.5, 40mM potassium acetate, 5mM $MgCl_2$ followed by incubation in Laemmli sample buffer at 70˚C for 10 minutes. Samples were analysed by SDS-PAGE and western blotting.

Mass spectrometry analysis

Mass spectrometry was performed at the Sanford-Burnham Proteomics Facility, Sanford-Burnham Medical Research Institute, (La Jolla) using the method previously described [50]. Briefly, beads from pull down assays were resuspended in a buffer containing 8M urea and 50mM ammonium bicarbonate followed by reduction with Tris(2-carboxyethyl) phosphine, (TCEP), alkylation with iodoacetamide and digestion with mass spectrometry grade trypsin (Promega). Samples were washed with 50mM ammonium bicarbonate and formic acid was added, followed by desalting. Peptides were analysed by high-resolution and high-accuracy LC-MS/MS. The LC-MS/MS raw data of three technical replicates were combined and submitted to Sorcerer Enterprise v.3.5 release (Sage-N Research Inc.) with SEQUEST algorithm as the search program for peptide/protein identification. The LC-MS/MS raw data were also submitted to Integrated Proteomics Pipelines (IP2) Version IP2 1.01 (Integrated Proteomics Applications, Inc.) with ProLucid algorithm as the search program for peptide/protein identification. ProLucid and SEQUEST were both set up to also search the target-decoy ipi. Human. v3.73 protein database. The search results were viewed, sorted, filtered, and statically analysed by using comprehensive proteomics data analysis software, Peptide/Protein prophet v.4.02 (ISB) and DTA Select for proteins. The differential spectral count analysis was done by QTools, an open-source tool for automated differential peptide/protein spectral count analysis and Gene Ontology. The reviewed human UniProt database was used for identifying SGTA interacting partners.

Preparation of HeLa lysate

HeLa M cells were plated in 10-cm dishes at 100% confluency and washed twice with PBS at 4˚C. Following washes, cells were lysed in a buffer containing 20mM HEPES pH 7.4, 5mM $MgCl_2$, 0.1M NaCl, 0.5% Triton x100, protease inhibitor and 1mM PMSF. Cells were harvested from the dish using a cell scrapper followed by incubation on ice for 10–15 minutes. The cell suspension was then centrifuged to remove cell debris at 13000 rpm at 4˚C for 20 min and the supernatant used for analysis.

Western blotting

Western blot experiments were performed according to standard procedures previously described [32]. Briefly, cells were lysed directly into Laemmli sample buffer and subjected to SDS-PAGE followed by infrared immunoblotting as described previously. Fluorescent bands for specific proteins were quantified using Image Studio-Lite (Li-Cor Biosciences) employing data from at least three independent experiments expressed as the mean ± s.e.m. The statistical significance of the results was assessed by applying a student's t-test using Prism 7 (GraphPad).

Co-immunoprecipitation

Stable HeLa Flp-In T-REx cell lines expressing OP91 or OpD were grown as detailed. Half of the samples were induced while the other half remained as uninduced samples. Cell lysates were prepared by harvesting cells in solubilisation buffer containing 10 mM Tris-HCl pH 7.4, 150 mM NaCl, 0.5% n-dodecyl β-D-maltopyranoside (DDM) and 1 mM EDTA supplemented with protease inhibitor tablets (Roche) and 1 mM PMSF for 1 hour at 4˚C. The lysates were centrifuged at 16,000 g for 20 minutes at 4˚C to remove insoluble material and 10% of the supernatant was retained as the input sample. Approximately 500 μL of the clarified lysate was incubated with IgG control or SGTA antibodies (1–2 μg) for 12 h at 4˚C with constant rotation. Protein A Sepharose (GenScript Biotech, Piscataway USA) was used to precipitate complexes by adding a 50% slurry and incubating for further 2 h. Beads were then washed five times in lysis buffer followed by elution of immune complexes by resuspending the beads in 2× Laemmli sample buffer followed by immunoblotting with appropriate antibodies.

Cycloheximide chase

Transfected HeLa Flp-In T-REx cells were treated with non-targeting siRNAi duplexes or siRNAi targeting USP5, USP9X, USP14, and SGTA as described above or transfected with USP5-HA, USP5-HA^{C335A}, SGTA-V5 or PEX19-V5 plasmids as previously described. Prior to harvesting transfected cells were treated with 100 μg/ml cycloheximide (Sigma, Aldrich) to inhibit protein synthesis. Cells were lysed directly into SDS-PAGE sample buffer at specific time-points followed by Western blotting analysis.

Results

Previous studies suggest that SGTA regulates the fate of membrane proteins that mislocalise to the cytosol [9, 32]. Overexpression of exogenous SGTA led to an increase in the steady-state levels of MLPs. One such model MLP is OP91, an N-terminal fragment of opsin that is inefficiently targeted to the endoplasmic reticulum [32]. SGTA also promoted the deubiquitination of MLPs [9, 32]. Since SGTA itself has no domains typical for DUBs, it was proposed that SGTA recruits one or more DUBs to exert these effects [9, 32, 43]. In this study we aimed to identify the DUBs that interact with SGTA in mammalian cells and dissect their role in MLP quality control.

Identification of SGTA interacting DUBs

To identify SGTA interacting DUBs, we took a proteomic based approach by isolating protein complexes that interact with SGTA using a pull-down assay. We made use of SGTA mutants that are defective in interacting with known SGTA binding partners to develop and validate a robust assay for the identification of specific SGTA interactors. The SGTA$^{K160E/R164E}$ mutant which does not interact with Hsp70 [48] and the SGTA$^{D27R/E30R}$ which does not interact with

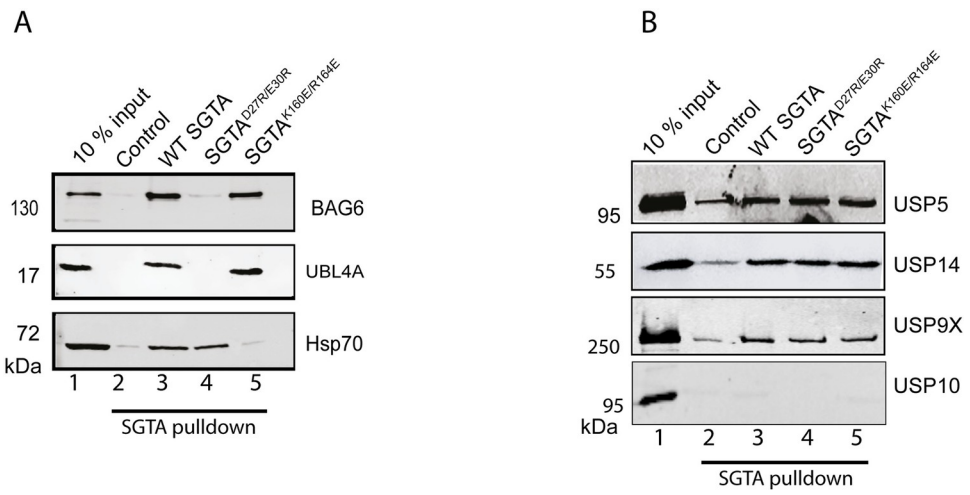

Fig 1. Identification of SGTA interacting DUBs. A) Beads coupled to recombinant Thioredoxin-SGTA fusion proteins as indicated or Thioredoxin only (Control) were incubated with rabbit reticulocyte lysate for 16 hours at 4˚C. The beads were washed as detailed in Materials and Methods. Twice the bead volume of SDS sample buffer was added, and samples were processed for SDS PAGE and Western blotting and probed with antibodies against Bag6, UBL4A and Hsp70 proteins using a fluorescence- based Odyssey ® Fc Imaging System (LICOR). **B)** Beads described in A, were incubated with HeLa lysate for 16 hours, washed and processed for Western blotting as detailed in A. Blots were probed with antibodies against USP5, USP14, USP9X and USP10 proteins using fluorescence- based detection on an Odyssey ® Fc Imaging System (LICOR).

https://doi.org/10.1371/journal.pone.0257786.g001

BAG6 and Ubl4A [20] were utilised in the pull-downs. WT SGTA, and the two SGTA mutants (SGTA$^{D27R/E30R}$ and SGTA$^{K160E/R164E}$) were purified as thioredoxin (TXN) fusion proteins and immobilised to UltraLink Biosupport beads. Immobilisation to beads allowed an equimolar input across all the pulldowns and enabled subsequent robust quantitative comparative analysis. Protein complexes interacting with these immobilised proteins were isolated from rabbit reticulocyte lysate under native conditions, with recombinant TXN immobilised to beads as negative control. The pull-downs were validated by Western blotting analysis, probing with BAG6, Ubl4A and Hsp70 specific antibodies. As expected, WT SGTA pulled-down high levels of BAG6, Ubl4A and Hsp70, while the TXN control did not pull-down any significant amounts of these three proteins (Fig 1A, cf. lanes 2 and 3). Consistent with previous publications [20], very low levels of BAG6 and Ubl4A were detected in the SGTA$^{D27R/E30R}$ mutant and Hsp70 levels were low in the SGTA$^{K160E/R164E}$ mutant (Fig 1A, cf. lanes 2, 3 and 4) [48].

Having validated that the pull-down approach was working as expected, pull-downs were performed as detailed above and the samples were analysed by mass spectrometry followed by interrogating the reviewed human UniProt database to identify SGTA interactors. Consistent with the Western blotting results (Fig 1A), beads containing WT SGTA were able to pull-down high levels of Bag6, Ubl4A and Hsp70 (Table 1) as judged from the spectral counts. The SGTA$^{D27R/E30R}$ mutant had very low spectral counts for Bag6 and Ubl4A, while the SGTA$^{K160E/R164E}$ mutant had very low levels of some isoforms of Hsp70, notably HspA2 known to specifically interact with SGTA [51]. Based on these results we gained confidence that this proteomic based approach was reliable and likely to reflect *bona fide* and novel SGTA interacting partners.

We then looked at all the DUBs that had been identified by mass spectrometry (Table 2). Based on spectra counts, USP5, USP9X, USP14, and USP7 were identified as candidates for follow-up studies (Table 2). Since our goal was to focus on the DUBs that play a role in the quality control of membrane proteins mislocalised to the cytosol, we looked in published

Table 1. SGTA interacting partners identified by mass spectrometry. Pull-down experiments were performed as described in Materials and Methods. The beads were then analysed for bound proteins by mass spectrometry as detailed in the materials and methods followed by interrogating the reviewed human UniProt database for SGTA interacting partners. Identified proteins known to interact with SGTA are indicated together with the spectral counts. SGTA peptides detected reflect comparative efficiency for the coupling of SGTA or the mutants to beads.

	Spectral counts			
SGTA interacting proteins	**Thrx**	**SGTA**	**SGTA$^{D27R/E30R}$**	**SGTA$^{K160E/R164E}$**
SGTA	28.8794	1813.40948	1799.50341	1561.96154
BAG6	70.6523	188.85411	26.81825	192.46266
HSPA2	96.34687	37.44345	34.27598	0
UBL4A	10.9873	15.07829	2.7107	17.22824
Number of SGTA peptides detected	28	1813	1753	1799

https://doi.org/10.1371/journal.pone.0257786.t001

literature for the subcellular localisation of the DUBs that we had identified. Based on this criteria USP7 was not included in further analysis as it is reported to localise mainly to the nucleus, while USP5, USP9X and USP14 localise to both the nucleus and cytosol [52].

Since the initial pull-downs which identified, these DUBs were performed using rabbit reticulocyte lysate we validated these results by repeating the pulldowns using lysate from HeLa cells. Pull-downs were performed as described above followed by Western blotting for the identified DUBs and USP10 which had very low spectral counts from the mass spectrometry results (Table 2). Consistent with the mass spectrometry data, WT SGTA and both mutants were able to pull down comparable amounts of USP5, USP9X, and USP14 when compared to TXN control, while USP10 was barely detectable, consistent with the very low spectral counts obtained for this DUB (Fig 1B, cf. lanes 2, 3, 4 and 5). From these results we decided to further investigate the role of USP5, USP9X, and USP14 in SGTA mediated quality control of MLPs.

Knocking down USP5 reduces the steady state of a model MLP

To investigate whether the identified DUBs play a role in MLP quality control, we reduced the level of endogenous DUBs using an siRNA approach and studied the effect on steady-state levels of the model MLP, OP91. We reasoned that if a DUB is responsible for the deubiquitination

Table 2. Putative SGTA interacting DUBs identified by mass spectrometry. Pull-down experiments were performed as described in Materials and Methods. The beads were then analysed for bound proteins by mass spectrometry as detailed in the materials and methods. All DUBs identified from the mass spectrometry are shown together with the spectral counts. The DUBs highlighted were prioritised for further studies based on high spectral counts and low background in the negative control.

	Spectral counts			
Putative SGTA interacting DUBs	**Thrx**	**SGTA**	**SGTA$^{D27R/E30R}$**	**SGTA$^{K160E/R164E}$**
Ubiquitin carboxyl-terminal hydrolase 10 [USP10]	0	0	0	0.36738
Ubiquitin carboxyl-terminal hydrolase 19 [USP19]	0	0	0.68318	0
Ubiquitin carboxyl-terminal hydrolase 5 [USP5]	**2.11094**	**9.27228**	**10.51442**	**8.43043**
Ubiquitin carboxyl-terminal hydrolase 14 [USP14]	**0**	**8.48274**	**14.24989**	**7.69728**
Ubiquitin carboxyl-terminal hydrolase 15 [USP15]	6.86995	7.72786	7.81252	6.96413
Ubiquitin carboxyl-terminal hydrolase 7 [USP7]	0	6.18345	5.75859	3.66414
Ubiquitin carboxyl-terminal hydrolase 47 [USP47]	0	1.5502	1.35755	0
Ubiquitin carboxyl-terminal hydrolase 32 [USP32]	0	1.53864	0	0.36577
Ubiquitin carboxyl-terminal hydrolase 4 [USP4]	0	1.1612	1.02477	0
Ubiquitin carboxyl-terminal hydrolase 24 [USP24]	0	0.77221	1.69914	0
Ubiquitin carboxyl-terminal hydrolase FAF-X [USP9X]	**0**	**5.40546**	**6.45057**	**4.39891**
Ubiquitin carboxyl-terminal hydrolase isozyme L5 [UCHL5]	0	1.93919	1.69474	0.36738
Ubiquitin thioesterase OTUB1 [OTUB1]	0	1.93341	1.35755	0

https://doi.org/10.1371/journal.pone.0257786.t002

and stabilisation of OP91, its knock down would enhance MLP degradation through favouring the ubiquitinated form which is subject to proteasomal clearance. Knocking down USP9X did not reduce the steady state levels of OP91 when compared to the non-targeting siRNAi (Fig 2A, lane 4), instead it led to a slight increase in the steady state levels of OP91 when signals were quantified and normalised to tubulin loading control (Fig 2B). Knocking down USP5 on the contrary led to a marked decrease in the steady state levels of non-glycosylated form [0-CHO] of OP91, suggesting a role on MLPs (Fig 2A, cf. lane 1 and 2). The significant changes in the OP91 signal were equivalent to ~50% reduction when compared to the non -targeting control (Fig 2B). Knockdown of USP14 also led to a decrease in the steady state levels of OP91, although the effect was less marked than that of USP5 (Fig 2A, cf. lane 1, 2 and 3), possibly because the knockdown of USP14 was less efficient. In these studies, knocking down any of these DUBs had no effect on SGTA levels (Fig 2A), suggesting these results are directly related to changes in levels of the DUBs. The effect of these DUBs was more apparent for the non-glycosylated form [0-CHO] of OP91, suggesting that they act on MLPs.

Mammalian USP14 and the yeast homologue, Ubp6 both associate with the proteasome [53, 54] and catalyse cleavage of ubiquitin subunits from substrates thereby delaying their proteasomal degradation [55]. OP91 was previously shown to be degraded by the proteasome [9, 32]. Hence, the destabilisation of OP91 upon knocking down USP14 is consistent with the effect of USP14 on proteasomal degradation of substrates. The destabilisation of MLPs upon USP5 knockdown is a novel finding that has not been previously reported. Hence, we focussed our attention on the role of USP5 in MLP quality control.

To validate the effects of USP5 on reducing the steady state levels of OP91, we made use of another siRNA oligonucleotide to independently target USP5. This siRNA oligonucleotide also led to a marked decrease in the level of OP91 (Fig 2C). The effect of reducing OP91 levels was reproducible as both siRNA oligonucleotides targeting USP5 led to ~ 50% reduction in OP91 levels (Fig 2D).

Loss of USP5 does not affect other substrates

Next, we wanted to confirm that the destabilisation effect observed after knocking down USP5 was specific for MLPs and not due to changes in ubiquitin homeostasis. To this effect, we made use of ubiquitin–methionine–GFP (Ub-M-GFP) which upon cleavage of ubiquitin does not have a degradation signal and is therefore stable [45] USP9X and USP14 were included in this experiment for comparison. Knocking down any of the DUBs did not affect the steady state levels of Ub-M-GFP (Fig 3A and 3B). We also made use of ubiquitin–arginine–GFP (Ub-R-GFP) [45] a proteasomal N-end rule substrate whose degradation was previously shown to be independent of SGTA [43]. Knocking down all the DUBs led to comparable steady-state levels of Ub-R-GFP (Fig 3A and 3B), suggesting the effects observed with USP5 are specific for OP91.

To further explore the substrate specificity of USP5, we looked at the effects of knocking down USP5 on the stability of the opsin degron (OpD), an ERAD substrate derived from wild-type opsin by the introduction of a degron motif into the first transmembrane domain [56]. The SGTA/ Bag6 complex was previously shown to play an important role in ERAD of OpD [20, 47] Knocking down USP5 did not change the steady state levels of OpD when compared to the non-targeting control (Fig 3C, cf. lane 1 and 2). On the other hand, knocking down USP14 and USP9X resulted in an accumulation of OpD (Fig 3C, cf. lane 1, 3 and 4). These effects mirrored what was observed when the proteasome is inhibited by Bortezomib (Fig 3C, lane 5). This observation is consistent with a perturbation of ERAD upon knocking down USP14 or USP9X but not USP5. Based on these results, we concluded that USP5 is a DUB that

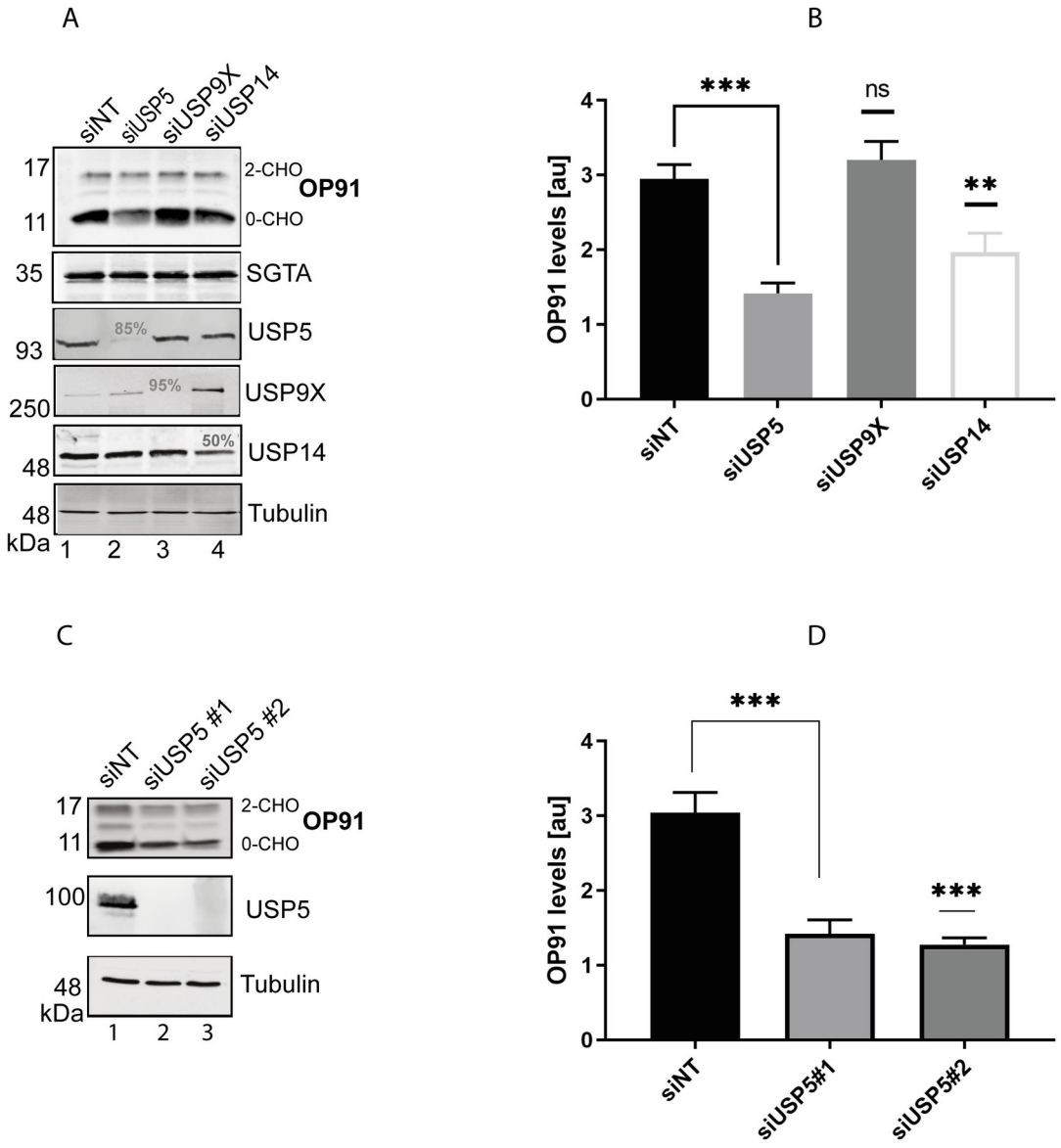

Fig 2. Knocking down USP5 reduces the steady state of a model MLP. A) HeLa TRex Flp-In cells stably expressing OP91 after induction, were seeded at 50% confluence and transfected with 1 nM of siRNAi targeting the indicated DUBs. OP91 expression was induced 48 h later and cells grown for 20 hrs post induction. Total cell lysates were prepared, and products analysed by Western blotting with antibodies against OP91, SGTA, USP5, USP9X, USP14 and tubulin (loading control) using fluorescence- based detection (LICOR). The % knockdown efficiency is indicated for each DUB in lane 2, 3 and 4. **B)** OP91 signals were quantified using Odyssey 2.1 software and normalised to the tubulin loading control, values show standard errors for n = 3. Pairwise comparisons relative to the NT control, were performed using GraphPad Prism. Student t-test: $P > 0.05$ = ns, $P \leq 0.05$ = *, $P \leq 0.01$ = **, $P \leq 0.001$ = *** **C)** HeLa TRex Flp-In cells stably expressing OP91 were transfected with non-targeting siRNAi or two independent siRNAi duplexes targeting USP5. Cells were treated as described in A, followed by blotting for OP91, USP5 and tubulin. **D)** OP91 signals were quantified using Odyssey ® Fc Imaging system and normalised to the tubulin loading control, values show standard errors for n = 3. Pairwise comparisons relative to the NT control, were performed using GraphPad Prism. Student t-test: $P > 0.05$ = ns, $P \leq 0.05$ = *, $P \leq 0.01$ = **, $P \leq 0.001$ = *** and $P \leq 0.0001$ = ****.

https://doi.org/10.1371/journal.pone.0257786.g002

plays a role in the cytosolic quality control of MLPs. It is plausible that initial capture of MLPs by SGTA may be similar between the cytosolic quality control and ERAD, however the triage process may be different, as this is likely driven by the different DUBs which determine ubiquitin chain editing and/or substrate localisation.

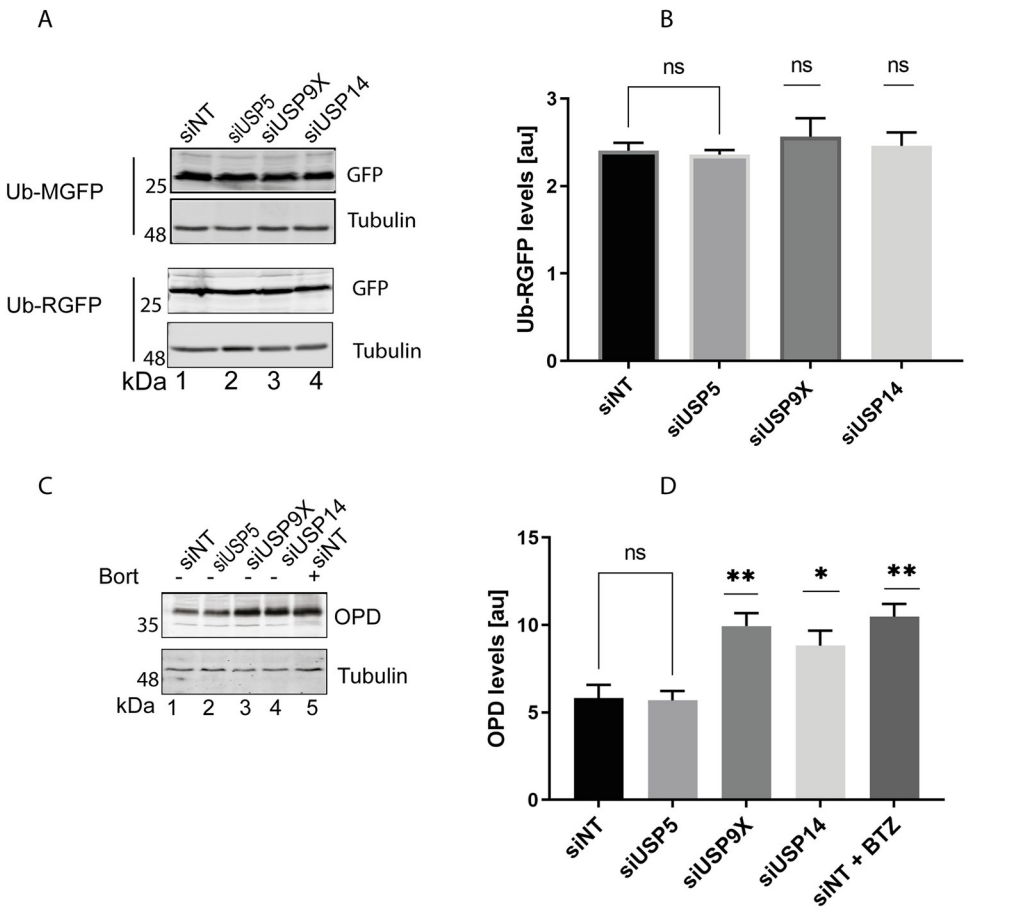

Fig 3. Loss of USP5 does not affect other substrates. A) HeLa M cells were seeded at 50% confluence and transfected with 1 nM of siRNAi targeting the indicated DUBs. Ub-MGFP and Ub-RGFP were transfected 48 h later and cells grown for 20 hrs post-transfection. Total cell lysates were prepared and analysed by Western blotting using GFP antibodies and tubulin (loading control). **B)** Ub-RGFP signals were quantified using the Odyssey ® Fc imaging system and normalised to the tubulin loading control, values show standard errors for n = 3. Pairwise comparisons relative to the NT control, were performed using GraphPad Prism. Student t-test: $P > 0.05$ = ns, $P \leq 0.05$ = *, $P \leq 0.01$ = **, $P \leq 0.001$ = ***. **C)** HeLa TRex Flp-In cells stably expressing OpD after induction were seeded at 50% confluence and transfected with 1 nM of siRNAi targeting the indicated DUBs. OpD expression was induced 48 h later, and cells grown for 20 hrs post induction. Total cell lysates were prepared and analysed by Western blotting using opsin antibodies to detect OpD, and tubulin (loading control). **D)** OP91 signals were quantified using Odyssey ® Fc imaging system and normalised to the tubulin loading control, values show standard errors for n = 3. Pairwise comparisons relative to the NT control, were performed using GraphPad Prism. Student t-test: $P > 0.05$ = ns, $P \leq 0.05$ = *, $P \leq 0.01$ = **, $P \leq 0.001$ = *** and $P \leq 0.0001$ = ****.

https://doi.org/10.1371/journal.pone.0257786.g003

USP5 protects OP91 against proteasomal degradation

Having established that knocking down USP5 reduces the steady state levels of OP91. We next investigated whether knocking down USP5 changes the OP91 mRNA levels. HeLa T-REx cells were transfected with oligonucleotides to knockdown USP5 or a non-targeting control. After 72 hours, cells were harvested and total RNA was extracted, followed by analysis of OP91 mRNA levels using quantitative RT-PCR. In contrast to the observed decrease in steady state levels of the OP91 protein, mRNA levels were comparable between the non-targeting control and a USP5 knockdown (Fig 4A), suggesting that the reduction in OP91 levels in a USP5 knockdown occurs post-translationally.

To further confirm that the changes in OP91 we see occur post-translationally, we made use of a series of combination knockdowns. Previous studies suggest that a BAG6/SGTA quality control cycle decide the fate of MLPs at the proteasome [43]. In this cycle, BAG6 antagonises the actions of SGTA by recruiting RNF126, which catalyses the selective ubiquitination of MLPs for subsequent degradation [31, 44]. Therefore, in the context of the BAG6/SGTA cycle, we reasoned that if the effect of USP5 on OP91 occurs post-translationally via this quality control cycle, knocking down BAG6 or RNF126, will negate or reduce the effects seen upon knocking down USP5, resulting in stabilisation of OP91. To this end we performed a series of combination knockdowns of USP5 with either, BAG6, SGTA or RNF126. Knocking down USP5 and SGTA, individually or together led to a reduction in OP91 levels (S1 Fig c.f. lanes 2, 3 and 4), consistent with their effect on antagonising BAG6 [9]. On the other hand, knocking down BAG6 or RNF126 alone (S1 Fig c.f. lanes 5 and 7) or in combination with USP5 (S1 Fig c.f. lanes 6 and 8) led to a stabilisation of OP91 when compared to knocking down USP5 alone. These results are consistent with the idea that in the absence of BAG6 or RNF126, OP91 ubiquitination will be lessened, hence its stabilisation. USP5 acts antagonistically to this reducing the level of stabilised OP91.

OP91 was previously shown to be degraded by the proteasome [32]. Therefore, we investigated whether OP91 was stabilised by proteasome inhibition when USP5 levels are reduced. Upon addition of Bortezomib, a proteasome inhibitor, there was an increase in steady state levels of OP91 in both the nontargeting control and in a USP5 knockdown (Fig 4B cf. lanes 2 and 5). Although, Leupeptin/Pepstatin which inhibits autophagy did not increase the steady state levels of OP91 in the non- targeting control (Fig 4B cf. lanes 3), this treatment led to stabilisation of a small proportion of OP91 in a USP5 knockdown (Fig 5B cf. lane 6). This observation suggests that in the absence of USP5 a small pool of OP91 is degraded by autophagy, consistent with the cross talk observed between the proteasomal and autophagic pathways of degradation [57].

To better understand the basis for the reduced steady-state levels of MLPs observed in a USP5 knockdown, we analysed OP91 levels over a 1-hour time course by blocking protein synthesis with cycloheximide and following degradation of OP91 in knockdowns of USP5, USP9X and in a nontargeting control. Previous studies showed that knocking down SGTA leads to a reduction in OP91 levels (S1 Fig cf. lane 2). We reasoned that if USP5 and SGTA act in the same pathway, their knockdown should affect the degradation of MLPs in a similar way. Therefore, an SGTA knockdown was included in the time-course experiments for comparison. Cycloheximide chase experiments revealed that in the non-targeting and USP9X knockdowns, ~50% of OP91 was degraded in the first 20 minutes with the rate of degradation slowing after this point (see S2A Fig). While, in the SGTA and USP5 knockdowns, there was a less marked reduction as the steady state levels of OP91 were already low before the start of the chase experiment (S2A Fig). Therefore, to better compare the degradation kinetics in these knockdowns, OP91 levels were expressed as a percentage of the total OP91 signal in the negative control (NT) at time zero (S2B Fig). This revealed similar degradation kinetics for all conditions, notably however, these experiments also revealed that when USP5 and SGTA are reduced there is loss of a protected pool of OP91 which is rapidly degraded.

Overexpression of USP5 stabilises OP91

To gain confidence of the role of USP5 in MLP quality control, we investigated the effect of overexpressing USP5 on the stability of OP91. To this end HA tagged USP5, and V5 tagged SGTA [43] were transfected into HeLa cells followed by induction of OP91 expression. We have previously shown that overexpression of a chaperone protein, Pex19 does not stabilise

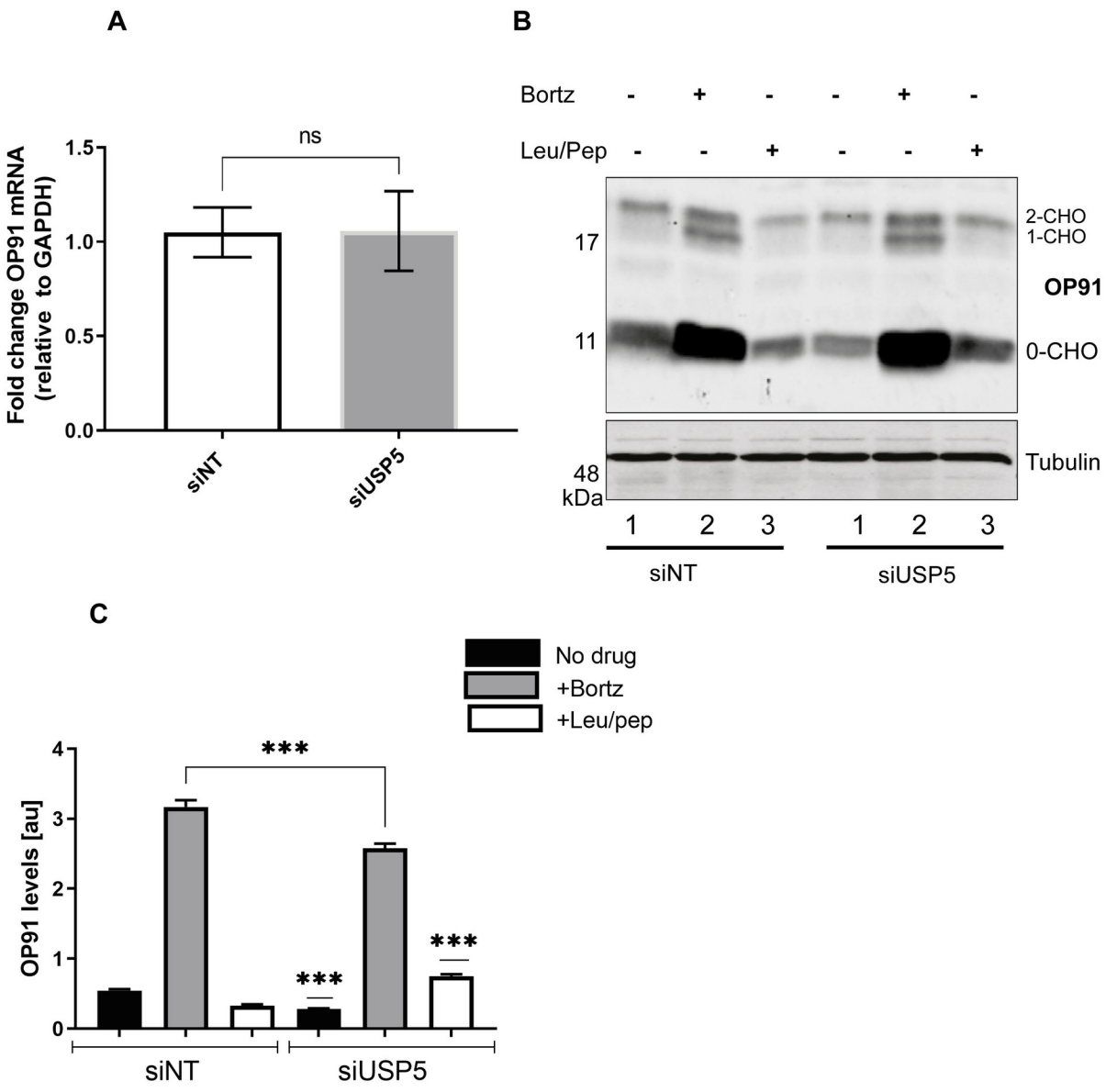

Fig 4. USP5 protects OP91 against proteasomal degradation. A) HeLa T-REx Flp-In cells stably expressing OP91 were seeded at 50% confluence followed by transfection of oligos for knockdown of USP5 or a non-targeting oligo. Cells were grown for 48 hrs followed by induction of OP91 expression and growth for a further 20 hrs post. Cells were harvested and total RNA extracted and used in a qPCR reaction following standard qPCR protocol. **B)** Cells grown as described in A, inhibitors of the proteasome and autophagy were added 24 hours before cells were harvested. Samples were analysed by SDS-PAGE and Western blotting for OP91 and Tubulin loading control. **C)** OP91 signals were quantified using Odyssey ® Fc Imaging System and normalised to the tubulin loading control, values show standard errors for n = 3. Pairwise comparisons were performed using GraphPad Prism. Student t-test: $P > 0.05$ = ns, $P \leq 0.05$ = *, $P \leq 0.01$ = **, $P \leq 0.001$ = *** and $P \leq 0.0001$ = ****.

https://doi.org/10.1371/journal.pone.0257786.g004

OP91 [43] Therefore, this was used as a negative control to reveal the basal level of OP91. After growth, cells were harvested into Laemmli sample buffer and analysed by Western blotting, probing for OP91, Tubulin, USP5, SGTA and PEX19. Consistent with previous studies [32, 43], overexpression of SGTA led to an increase in the steady state levels of OP91 (Fig 5A cf. lane 2), above those seen in the presence of exogenous PEX19 control (Fig 5A cf. lane 1). Over-expression of USP5 led to 2-fold increase in the steady state levels of OP91 when compared to

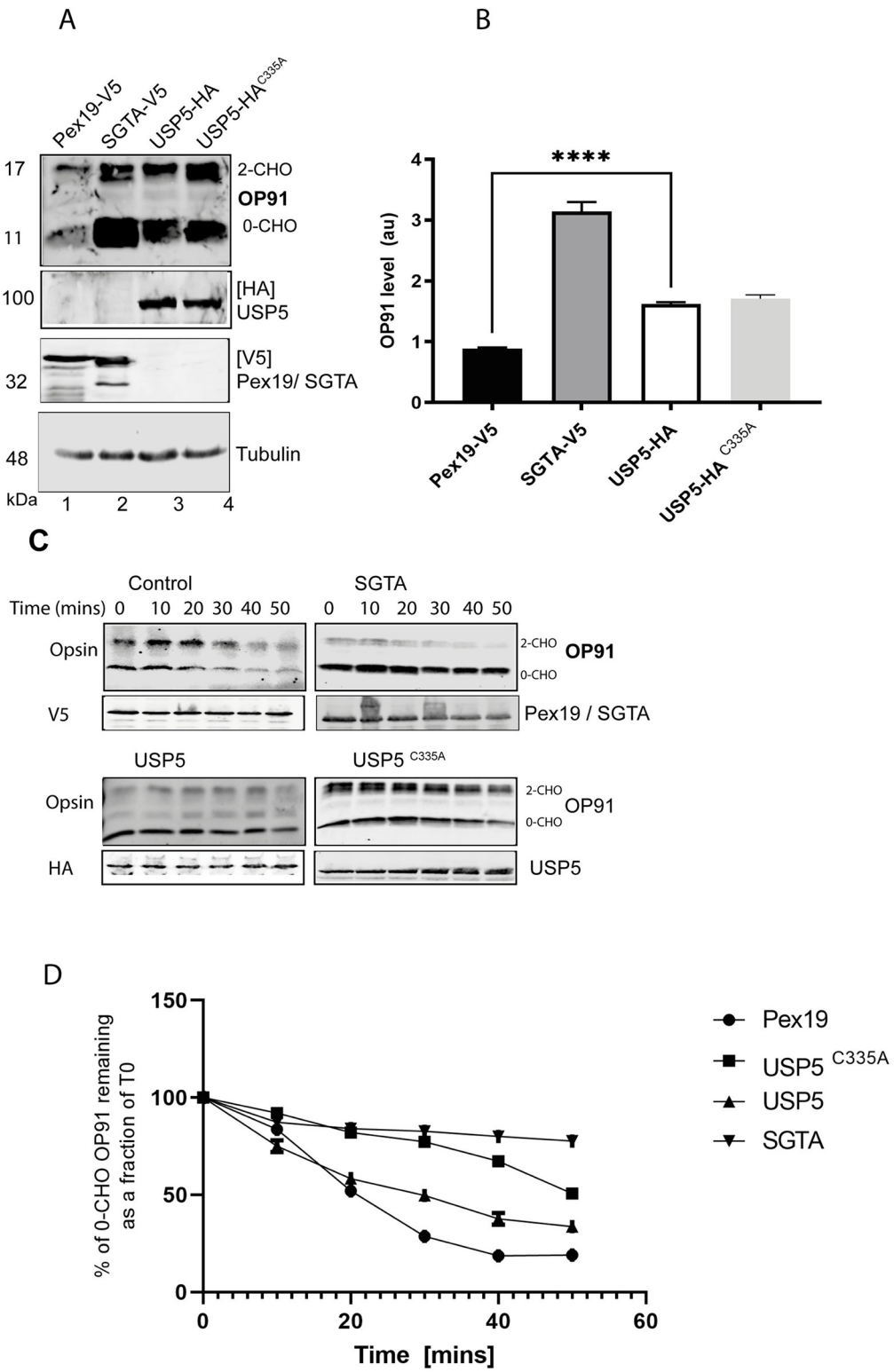

Fig 5. Overexpression of USP5 stabilises OP91. A) HeLa T-REx Flp-In cells stably expressing OP91 upon induction were transfected with V5-tagged Pex19 and SGTA or HA -tagged WT or C335A mutant of USP5. OP91 expression was induced 6 hours post-transfection. Cells were grown for a further 20 hours, post-induction. Total cell lysates were prepared and analysed by western blotting using antibodies against OP91, V5 tagged SGTA and Pex19, HA tagged USP5 and USP5^{C335A} and tubulin (loading control). **B)** OP91 signals were quantified using Odyssey ® Fc Imaging

System and normalised to the tubulin loading control, values show standard errors for n = 3. **C)** HeLa T-REx Flp-In cells stably expressing OP91 upon induction were transfected with plasmids encoding V5-tagged Pex19 and SGTA or HA -tagged WT USP5 or USP5^{C335A}. OP91 expression was induced by addition of medium containing 1 μg/ml of tetracycline and grown for 20 hrs post induction. Prior to harvesting transfected cells were treated with 100 μg/ml cycloheximide (Sigma, Aldrich) to inhibit protein synthesis. Cells were lysed directly into SDS-PAGE sample buffer at indicated time-points followed by Western blotting with antibodies against opsin (OP91), HA (USP5 and USP5^{C335A}), V5 (SGTA and Pex19) and tubulin (loading control) using fluorescence- based detection (LICOR). **D)** OP91 signal for each condition was quantified and plotted against the respective time points.

https://doi.org/10.1371/journal.pone.0257786.g005

the Pex19 control (Fig 5A cf. lane 3 and Fig 5B). We also made use of the C335A catalytic mutant of USP5 which binds but does not hydrolyse ubiquitin conjugates [58–60]. Overexpression of this mutant also resulted in a 2-fold increase in the steady state levels of OP91 (Fig 5A cf. lane 4 and Fig 5B). These results are consistent with the previously reported dominant negative effect of this mutant as it binds and sequesters the substrate, protecting it from degradation and thus leading to stabilisation [58–60]. Overall, these results demonstrated that modulating USP5 levels directly affect MLP quality control.

Having shown that USP5 and the C335A mutant stabilise OP91, we next investigated whether this stabilisation is due to a delay in degradation. To this end, we expressed these constructs in HeLa cells and performed a cycloheximide chase experiment. Overexpression of the C335A catalytic mutant of USP5 resulted in a marked delay in degradation of OP91 (Fig 5C and 5D). Moreover, when the non-glycosylated [0-CHO] band, which reflects untranslocated OP91 was quantified, both the WT USP5 and the C335A mutant of USP5 led to a delay in degradation when compared to cells transfected with Pex19 control, as judged by signal intensity of OP91 at each time point relative to that of the control (Fig 5C and 5D). These observation mirror closely what was observed for the overexpression of SGTA which also delayed degradation of OP91 in a cycloheximide chase experiment as indicated (Fig 5C and 5D) [32].

USP5 specifically enhances SGTA activity

It was previously shown that increasing exogenous SGTA levels leads to an increase in steady state levels of OP91 [32, 43]. Having shown that USP5 is also required for the stabilisation of OP91 in this study (Fig 2A & 2B), we next asked whether the stabilising effect of SGTA is dependent on USP5. To this end we performed a knockdown of USP5 and used non-targeting siRNAi as control. After 48 hours, V5 tagged SGTA or Pex19 control were transfected followed by induction of OP91 expression. After growth, cells were analysed by Western blotting for OP91, tubulin, and V5 tagged SGTA or Pex19. Overexpression of SGTA led to stabilisation of OP91 in the presence of the nontargeting siRNAi (Fig 6A cf. lane 2), when compared to the Pex19 control (Fig 6A cf. lane 1). However, in the presence of USP5 siRNAi, overexpression of SGTA did not stabilise OP91 to the same level as observed in the presence of non-targeting siRNAi (Fig 6A cf. lane 2 and 4), suggesting that USP5 is required for the stabilisation of OP91 observed during SGTA overexpression.

We also revisited the effect we observed that upon knockdown of USP14 destabilisation of OP91 occurred (Fig 2A). To investigate whether USP14 is required for the stabilisation effect observed with exogenous SGTA, we knocked down USP14 and overexpressed SGTA. We also looked at the effects in a USP9X knockdown as this did not affect the steady state levels of OP91 (Fig 2A & 2B). As expected, reducing USP9X did not affect the ability of SGTA to stabilise OP91 (Fig 6C cf. lane 5 and 6). On the other hand, lack of USP5 led to a reduction in the ability of SGTA to stabilise OP91 (Fig 6C cf. lane 3 and 4). However, the knockdown of USP14 did not affect the ability of exogenous SGTA to stabilise OP91 (Fig 6C cf. lane 7 and 8), suggesting that USP14 is not directly required for the SGTA mediated stabilisation of OP91.

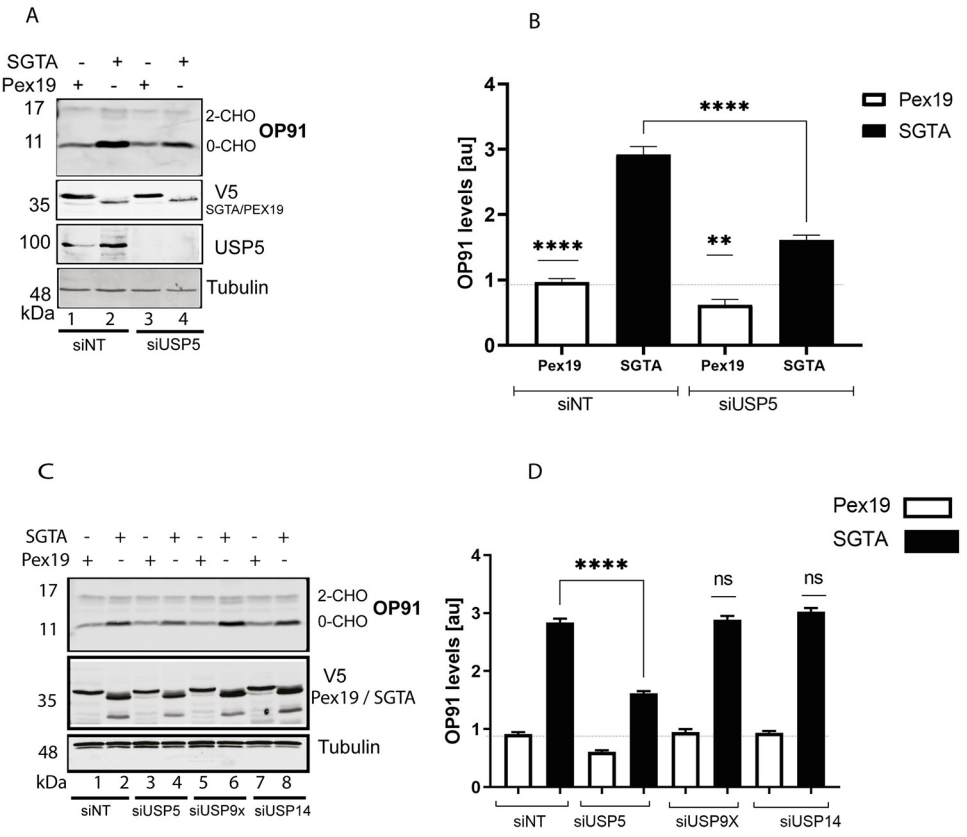

Fig 6. USP5 specifically enhances SGTA activity. A) HeLa T-REx Flp-In cells stably expressing OP91 after induction were seeded at 50% confluence and transfected with 1 nM of siRNAi targeting USP5 or a nontargeting control and incubated for 48 hours. After this, plasmids expressing V5 tagged SGTA or PEX19 were transfected followed by incubation for 6 hours before the medium was replaced with medium containing 1 mg/ml of tetracycline to induce OP91 expression. Cells were grown for 20 hrs post induction and total cell lysate were prepared and products analysed by western blotting using antibodies for opsin (OP91), V5 (SGTA and PEX19), and tubulin (loading control). **B)** OP91 signals were quantified using Odyssey ® Fc Imaging System and normalised to the tubulin loading control, values show standard errors for n = 3. Pairwise comparisons relative to Pex19, were performed using GraphPad Prism. Student t-test: $P > 0.05$ = ns, $P \leq 0.05$ = *, $P \leq 0.01$ = **, $P \leq 0.001$ = *** and $P \leq 0.0001$ = ****. **C)** HeLa T-REx Flp-In cells were treated with siRNAi targeting USP5, USP9X, USP14 and a nontargeting control and analysed as detailed in A. **D)** OP91 signals were quantified using Odyssey ® Fc Imaging System and normalised to the tubulin loading control, values show standard errors for n = 3. Pairwise comparisons relative to Pex19, were performed using GraphPad Prism. Student t-test: $P > 0.05$ = ns, $P \leq 0.05$ = *, $P \leq 0.01$ = **, $P \leq 0.001$ = *** and $P \leq 0.0001$ = ****.

https://doi.org/10.1371/journal.pone.0257786.g006

Association of SGTA and USP5 is enhanced in the presence of an MLP

Co-immunoprecipitation studies have shown that SGTA and OP91 are in a complex [32]. We next wanted to see whether USP5 was also part of this complex. To this effect, HeLa cells were grown and induced to express OP91 in half of the samples. After growth, cells were harvested into non-denaturing buffer and subjected to co-immunoprecipitation using SGTA antibodies or IgG antibodies as negative control. Endogenous SGTA associated with USP5 in the absence of OP91 induction and this association was increased upon OP91 induction (Fig 7A cf. lane 5 and 6), suggesting that association of USP5 and SGTA is substrate dependent. The endogenous SGTA coimmunoprecipitated with the non-glycosylated form [0-CHO] of OP91 which reflects the mislocalised form. Since the IgG control did not show an increased association of USP5 with endogenous SGTA even upon OP91 induction (Fig 7A cf. lane 3 and 4), these results suggested that this association was specific for SGTA.

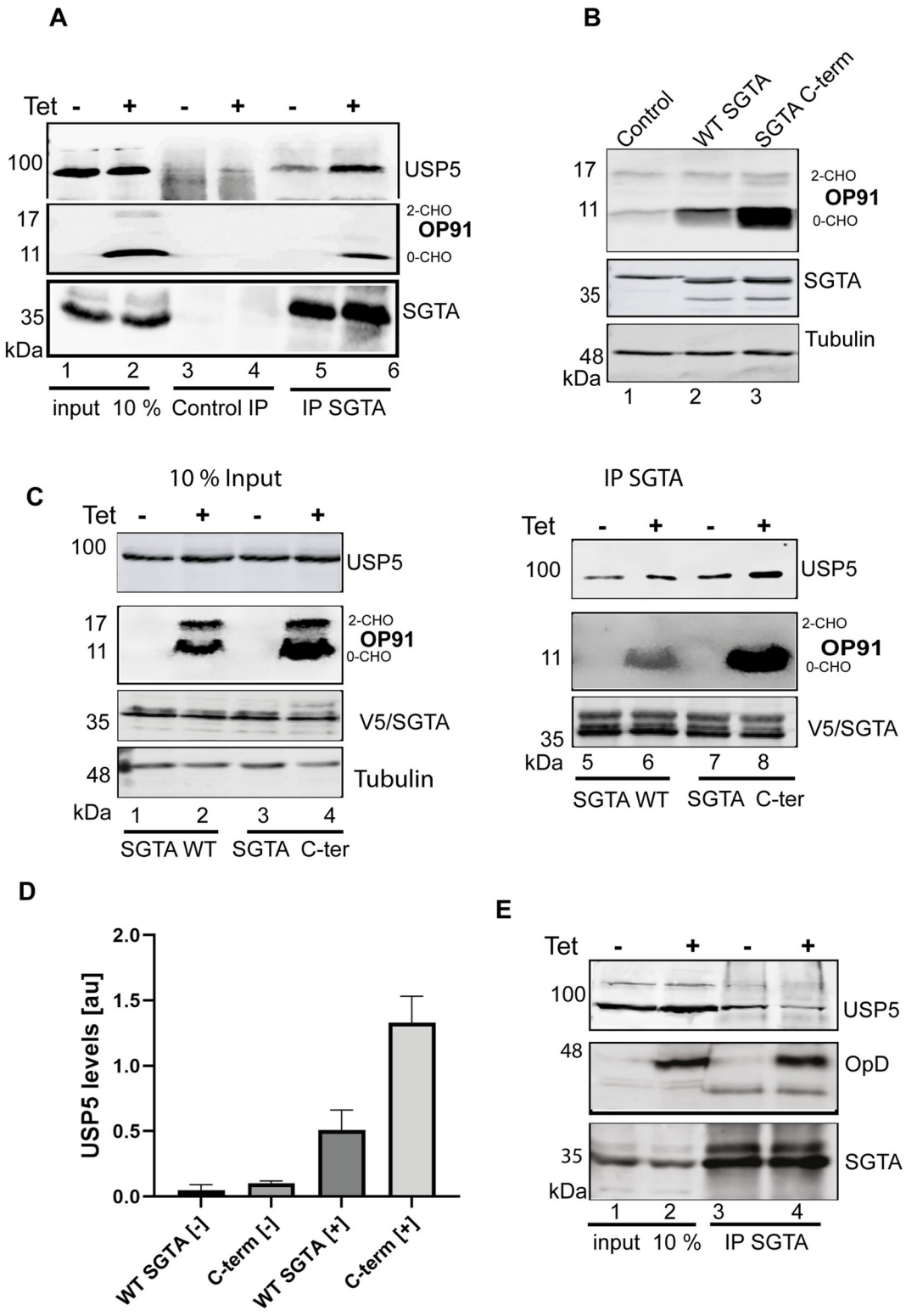

Fig 7. Association of SGTA and USP5 is enhanced in the presence of an MLP. A) HeLa T-REx Flp-In cells stably expressing OP91 after induction were seeded at 50% confluence and induced to express OP91 in half of the samples. After growth, cells were harvested into non-denaturing buffer and subjected to co-immunoprecipitation using SGTA antibodies or IgG antibodies as negative control. Products were analysed by western blotting using antibodies against opsin (OP91), V5 (SGTA) and tubulin (loading control). **B)** HeLa TRex Flp-In cells stably expressing OP91 after induction were transfected

with V5 tagged WT SGTA or SGTA-3xNNP/AAA C-terminal mutant (denoted here as SGTA C-term) followed by incubation for 6 hours before the medium was replaced with medium containing 1 mg/ml of tetracycline to induce OP91 expression. Cells were grown for 20 hrs post induction and total cell lysate were prepared and products analysed by western blotting using antibodies for opsin (OP91), V5 (SGTA and SGTA- C-term), and tubulin (loading control). **C)** Cells transfected with WT SGTA or the SGTA C-terminal mutant described in B were processed for immunoprecipitation using SGTA antibodies. Samples were analysed by western blotting using antibodies against SGTA, OP91 and USP5. **D)** USP5 signals in the IP lanes 5–8 were quantified using Odyssey ® Fc Imaging System and normalised to the tubulin loading control, values show standard errors for n = 3. Pairwise comparisons of the induced [+] relative to the uninduced [−], were performed using GraphPad Prism. Student t-test: $P > 0.05$ = ns, $P \leq 0.05$ = *, $P \leq 0.01$ = **, $P \leq 0.001$ = *** and $P \leq 0.0001$ = ****. **E)** HeLa TRex Flp-In cells stably expressing OpD upon induction were seeded at 50% confluence and grown to 80% confluency followed by induction of OpD expression in half of the samples. Cells were subjected to immunoprecipitation as detailed in A.

https://doi.org/10.1371/journal.pone.0257786.g007

SGTA contains a well conserved C-terminal NNP region characterized by three repeats of the NNP motif. Previously, a mutant version of SGTA in which all three NNP motifs were altered to alanine's (SGTA-3xNNP/AAA-V5), was shown to enhance the ability of SGTA to stabilise OP91 five-fold [46], (Fig 7B, cf. lane 2 and 3). To further investigate the substrate dependent association of SGTA and USP5 we made use of this SGTA mutant. We reasoned that if the stabilisation of MLPs is linked to USP5, this mutant will likely associate with more USP5 than WT SGTA. We therefore asked whether this mutant associates with more USP5 compared to the WT SGTA. To this end, HeLa cells were transfected with V5 tagged WT SGTA or the SGTA mutant, followed by induction of OP91 expression in half of the samples. Cells were harvested into non-denaturing buffer 24 hours post-induction and subjected to co-immunoprecipitation using SGTA antibodies or IgG antibodies as a negative control. As expected SGTA associated with USP5 in the absence of OP91 induction and this association was increased upon OP91 induction (Fig 7C cf. lane 3 and 4). Similarly, the SGTA-3xNNP/AAA mutant associated with more USP5 in the absence of induction (Fig 7C cf. compare lane 1 and 3), consistent with an increase in stabilisation of OP91 seen in this mutant before induction. Upon induction of OP91, there was an increase in association compared to the WT (Fig 7C cf. compare lane 2 and 4), which led to a 3-fold increase in USP5 (Fig 7D), concomitant with an increase in OP91. Therefore, these results strongly suggested that this association is substrate dependent. We also looked at whether the stabilisation of OP91 in the SGTA-3xNNP/AAA mutant requires USP5. Consistent with the results in Fig 6, knocking down USP5 in this mutant resulted in a 3-fold reduction in OP91 levels (S3A and S3B Fig), suggesting that in this mutant the stabilisation of OP91 is largely linked to the presence of USP5.

To validate these observations, we investigated the association of SGTA and USP5 in the presence of the ERAD substrate, opsin degron (OpD) [20, 47]. Induction of OpD did not result in an increase in the association of endogenous SGTA and USP5 when compared to the uninduced sample (Fig 7E, cf. lane 3 and 4). Based on these results, we concluded that association of USP5 and SGTA is specifically enhanced by the presence of an MLP. Attempts to confirm direct binding of SGTA to USP5 *in vitro* did not show direct binding, suggesting the interaction may be via an adaptor protein.

Discussion

A role for DUBs in SGTA mediated protein quality control was first apparent when SGTA was reported to promote deubiquitination of MLPs [9, 32]. However, until now the deubiquitinating enzymes that play a role in this process had not been identified. In this study, we identified DUBs associated with SGTA by using pull-down assays and mass spectrometry. We confirmed that knocking down USP5 specifically reduces the steady state levels of a model MLP (Fig 2), while overexpression of USP5 leads to an increase (Fig 5). Using co-immunoprecipitation, we

show an association of USP5 and SGTA which is dependent on the presence of an MLP: association of USP5 with SGTA was increased upon induction of OP91 (Fig 7). This association is specific for MLPs as we did not observe an increase in the association of USP5 with OpD, an ERAD substrate (Fig 7). Moreover, a gain of function mutant of SGTA which leads to a 20-fold increase in the steady state levels of OP91 (Fig 7) showed increased USP5 association when compared to WT SGTA (Fig 7). The failure of SGTA to effectively stabilise OP91 in the absence of USP5 (Fig 6) points to an important role of USP5 in SGTA mediated quality control of membrane proteins that mislocalise to the cytosol. This is supported by an increased association of USP5 with the non-glycosylated OP91 which is mislocalised but has not been ER translocated (Fig 7).

The results in Fig 7A show that USP5 associates with endogenous SGTA, and this association is increased upon induction of OP91, suggesting that the association of SGTA and USP5 is substrate dependent. The SGTA C-terminal mutant caused increased stabilisation of OP91; suggesting that in this mutant the increased association of USP5 with SGTA is also largely driven by the substrate. In Fig 6, we showed that USP5 is required for SGTA to efficiently stabilise OP91. In the C-terminal mutant, we also found that the levels of OP91 were reduced in a USP5 knockdown, and not significantly different from WT SGTA under the same conditions. This strongly suggests that USP5 is key to the stabilisation effect of OP91 in both SGTA and the C-terminal mutant. However, since we do not know the mode of binding and have not identified a binding site of USP5 on SGTA, we cannot rule out a direct effect of the mutant on USP5 binding. In addition, Fig 5 shows that both the WT and the catalytic mutant of USP5 stabilise OP91. Hence, it is not possible based on these results to make a conclusion on whether the catalytic activity of USP5 is required for its role in MLP quality control. Clarifying these questions is part of our current research efforts.

USP5 has a well characterised function regulating a stable pool of free ubiquitin in vivo by recycling unanchored polyubiquitin chains [13, 61, 62]. In this regard, USP5 hydrolyses K63-, K48-, K11-, K29- linked and linear polyubiquitin chains [63]. However, it is becoming clear that a wide range of physiological and pathological processes are regulated via USP5-mediated deubiquitination of various substrates [64]. For example, overexpression of USP5 was shown to stabilise FoxM1, a protein with a key role in tumorigenesis and progression of pancreatic cancers [65]. In addition, USP5 was shown to associate with the linker III-IV of the Cav3.2 protein and its knockdown increased ubiquitination of Cav3.2 protein and subsequent degradation, thus supporting the notion that USP5 stabilises Cav3.2 [66]. Moreover, USP5 was recently shown to play a critical role in epithelial-mesenchymal transition (EMT) of hepatocellular carcinoma by regulating levels of the transcription factor, SLUG. In this regard, knockdown of USP5 inhibits SLUG deubiquitination, while overexpression of USP5 promotes SLUG stability and EMT in vitro and in vivo [67]. In glioblastoma multiforme, USP5 plays a critical role in tumorigenesis and progression by stabilizing CyclinD1 protein [68]. USP5 also deubiquitinates and stabilizes c-Maf, a transcription factor related to tumor and immune cell differentiation and suppresses apoptosis in multiple myeloma cells [69]. Hence, a role of USP5 in regulating MLP levels is consistent with these observations.

USP5 shares 54.8% sequence identity with USP13, hence a partial functional overlap between the two has been suggested. Indeed, USP5 and USP13 are both recruited to stress granules containing K48 and K63 linked ubiquitin chains. In this case, depletion of USP5 and USP13 led to an increase in ubiquitinated proteins in heat induced stress granules, suggesting these DUBs play a role in ubiquitin editing of substrates to facilitate disassembly of stress granules [70]. Despite these functional overlaps, there is evidence supporting the idea that these closely related DUBs also have some distinct roles and classes of substrates. For instance, USP13 was previously shown to promote a stable interaction between BAG6 and SGTA during

ERAD and its knockdown reduced this interaction [20]. On the other hand, USP5 did not have a direct effect on the interaction of SGTA and BAG6 [20]. Consistent with these observations, in this study we did not observe an effect of USP5 on the stability of the opsin degron, an ERAD substrate. Moreover, in our pulldown assays, we did not detect an association of SGTA with USP13, suggesting USP13 might have a limited or no role in MLP quality control.

Our results clearly indicate that USP5 enhances SGTA mediated MLP quality control: the ability of SGTA to stabilise MLP was significantly reduced in the absence of USP5 (Fig 6). However, it is not clear how USP5 exerts these effects. This is complicated by the fact that DUBs such as USP5 have many cellular targets. Therefore, the effects of USP5 may be indirect as was reported for USP13 [21]. It was shown that, USP13 prevents promiscuous gp78-mediated ubiquitination of Ubl4A, a BAG6 cofactor which promotes ERAD. Ubiquitination of Ubl4A was accompanied by irreversible cleavage of BAG6 and attenuation of ERAD [21]. Hence, the deubiquitination action of USP13 eliminates ubiquitin conjugates from Ubl4A to maintain the function of BAG6, thereby ensuring efficient disposal of ERAD substrates. Recently, it was also shown that USP13 and gp78 also regulate the caspase activity of CASP3, which cleaves BAG6 and switches its function from an ERAD regulator to an autophagy tuner [19]. It was shown that the LIR1 motif of BAG6 holds the autophagosome structural membrane proteins LC3B-I and the unprocessed form of LC3B to suppress autophagy. This inhibition is relieved by the ubiquitination of thioredoxin which results in CASP3 activation and cleavage of BAG6 [19]. Hence, it may be that USP5 might exerts its' effects by modulating the ubiquitination status of a key player in the degradation pathway of MLPs rather than the MLP itself. Reconstitution of the DUB reaction *in vitro* is necessary in order to fully defined the role of USP5 in MLP quality control.

Functional pairing of E3 ligases with DUBs, as discussed for gp78 and USP13, is an important regulatory step in protein quality control [15]. In MLP quality control, BAG6 binds hydrophobic substrates and recruits RNF126, an E3 ubiquitin ligase which catalyses the selective ubiquitination of MLPs [31, 44]. On the other hand, DUBs such as USP5 promote substrate deubiquitination thereby giving substrates a chance to avoid proteasomal degradation [9, 32, 43]. Hence, future work should study the interplay of USP5 and RNF126 in regulating MLP quality control. Another possibility is that USP5 might play a key role in ubiquitin chain editing, by promoting K-63 linked assembly of substrates which would favour their accumulation in inclusion bodies. This would be the reverse of what is seen with the DUBs, Ubp2 and Ubp3 which prevent assemble of K-63 chains on substrates thereby promoting K-48 mediated proteasomal degradation [18]. To understand the role of USP5 in MLP quality control, it is necessary to study the type of ubiquitin linkages of MLPs and how these change upon rapid depletion of USP5 by using approaches such as the auxin-inducible degron (AID) technology [71].

In this study we did not detect a direct interaction of USP5 and SGTA, suggesting the interaction might be via an adaptor protein. A key role of the adaptor protein UBXN1 in regulating the interaction of VCP with BAG6 clients occurring prior to ER insertion was recently demonstrated [72]. It was shown that BAG6 clients, once ubiquitylated, were not directly degraded by the proteasome, but were recognised by the VCP-UBXN1 complex prior to degradation. Failure of ubiquitinated substrates to engage the UBXN1 adaptor led to their accumulation as aggregates [72], underscoring the importance of the adaptor proteins in protein quality control. In the case of USP5, the dendritic cell-derived ubiquitin (Ub)-like protein (DC-UbP) functions as an adaptor protein reconciling the cellular ubiquitination and deubiquitination processes by regulating the function of USP5 and UbE1 [73]. The C-terminal UbL domain of DC-UbP interacts with the UBA domains of USP5 and with the Ub-fold domain (UFD) of the Ub-activating enzyme UbE1, on the distinct surfaces. Overexpression of DC-UbP enhanced

the association of these two enzymes and prompted cellular ubiquitination, whereas knockdown of the protein reduced the cellular ubiquitination level [73]. In the case of MLP quality control, SGTA may function in a similar way to DC-UbP as it has a ubiquitin (Ub)-like domain on the N-terminus where BAG6 binds and promote RNF126 recruitment [31]. It may be that this (Ub)-like domain also promotes recruitment of DUBs such as USP5, via another protein. Future work should investigate the nature of interaction between USP5 and SGTA and identify any adaptor proteins involved in this process.

The number of DUBs that play important roles in the cytosolic protein quality control continues to increase, and this study adds USP5 to this list. This study suggests that USP5 impacts on the disposal of MLPs and possibly other aggregation prone proteins when its levels are modulated. Therefore, future work should extend these studies to other membrane proteins and to substrates implicated in pathologies such as neurodegeneration and cancer in order to understand how USP5 regulates their fates. These studies will shed light on how USP5 can be modulated as a therapeutic target for prevention of terminal aggregates which are linked to neurodegenerative diseases, cancer, and type II diabetes. The apparent specificity of USP5 for cytosolic substrates, makes effective therapies more likely as there may be a limited crosstalk to other DUBs and pathways.

Supporting information

S1 Fig. Knockdown of Bag6 or RNF126 is antagonistic to USP5. HeLa T-REx Flp-In cells stably expressing OP91 after induction were seeded at 50% confluence and transfected with 1 nM of siRNAi targeting either USP5, SGTA, BAG6 or RNF126 alone or in the combinations indicated. A nontargeting siRNAi was used as a negative control. After 48 hrs, OP91 expression was induced by replacing with medium containing 1 mg/ml of tetracycline. Cells were grown for 20 hrs post induction and total cell lysate were prepared and analysed by western blotting using antibodies for opsin (OP91), SGTA, USP5, BAG6 and tubulin (loading control) and detected using an Odyssey ® Fc imaging system. The siRNAi for RNF126, though not validated here was extensively used in previous studies [31].
(TIF)

S2 Fig. USP5 and SGTA protect OP91 from degradation. A) HeLa T-REx Flp-In cells stably expressing OP91 were seeded at 50% confluence and transfected with 1 nM of siRNAi targeting USP5, USP9X, SGTA or a nontargeting control and incubated for 48 hours. After this OP91 expression was induced by addition of medium containing 1 μg/ml of tetracycline and grown for 20 hrs post induction. Prior to harvesting transfected cells were treated with 100 μg/ml cycloheximide (Sigma, Aldrich) to inhibit protein synthesis. Cells were lysed directly into SDS-PAGE sample buffer at specific time-points followed by Western blotting with antibodies against opsin (OP91) and tubulin (loading control) using fluorescence- based detection (LICOR). **B)** OP91 signals were quantified using Odyssey ® Fc imaging system and normalised to the tubulin loading control, values show standard errors for n = 3.
(TIF)

S3 Fig. USP5 is required for stabilisation of OP91 in the presence of SGTA C-terminal mutant. A) HeLa T-REx Flp-In cells stably expressing OP91 were seeded at 50% confluence and transfected with 1 nM of siRNAi targeting USP5 or a nontargeting control and incubated for 48 hours. Following this, cells were transfected with V5 tagged WT SGTA or SGTA-3xNNP/AAA C-terminal mutant (denoted here as SGTA C-term) followed by incubation for 6 hours before the medium was replaced with medium containing 1 mg/ml of tetracycline to induce OP91 expression. Cells were grown for 20 hrs post induction and total cell lysate were

prepared and products analysed by western blotting using antibodies for opsin (OP91), V5 (SGTA and SGTA- C-term), and tubulin (loading control). **B)** OP91 signals were quantified using Odyssey ® Fc imaging system and normalised to the tubulin loading control, values show standard errors for n = 3.
(TIF)

S1 Raw images.
(PDF)

Acknowledgments

We thank Prof. Stephen High for his guidance and support with reagents and manuscript preparation, without his input this work would not have been possible. Dr Pawel Leznicki for proofreading and advice during the preparation of this manuscript.

Author Contributions

Conceptualization: Yvonne Nyathi.

Data curation: Jake Hill, Yvonne Nyathi.

Formal analysis: Jake Hill, Yvonne Nyathi.

Funding acquisition: Yvonne Nyathi.

Investigation: Jake Hill, Yvonne Nyathi.

Methodology: Yvonne Nyathi.

Project administration: Yvonne Nyathi.

Resources: Yvonne Nyathi.

Supervision: Yvonne Nyathi.

Validation: Yvonne Nyathi.

Visualization: Yvonne Nyathi.

Writing – original draft: Yvonne Nyathi.

Writing – review & editing: Jake Hill, Yvonne Nyathi.

References

1. Shao S, Rodrigo-Brenni MC, Kivlen MH, Hegde RS. Mechanistic basis for a molecular triage reaction. Science. 2017; 355(6322):298. https://doi.org/10.1126/science.aah6130 PMID: 28104892
2. Bayer TA. Proteinopathies, a core concept for understanding and ultimately treating degenerative disorders? European Neuropsychopharmacology. 2015; 25(5):713–24. https://doi.org/10.1016/j.euroneuro.2013.03.007 PMID: 23642796
3. Dubnikov T, Ben-Gedalya T, Cohen E. Protein Quality Control in Health and Disease. Cold Spring Harb Perspect Biol. 2017; 9(3). Epub 2016/11/20. https://doi.org/10.1101/cshperspect.a023523 PMID: 27864315
4. Hessa T, Sharma A, Mariappan M, Eshleman HD, Gutierrez E, Hegde RS. Protein targeting and degradation are coupled for elimination of mislocalized proteins. Nature. 2011; 475:394. https://doi.org/10.1038/nature10181 PMID: 21743475
5. Stolz A, Wolf DH. Endoplasmic reticulum associated protein degradation: A chaperone assisted journey to hell. Biochimica et Biophysica Acta (BBA)—Molecular Cell Research. 2010; 1803(6):694–705. https://doi.org/10.1016/j.bbamcr.2010.02.005 PMID: 20219571

6. Ast T, Aviram N, Chuartzman SG, Schuldiner M. A cytosolic degradation pathway, prERAD, monitors pre-inserted secretory pathway proteins. Journal of Cell Science. 2014; 127(14):3017. https://doi.org/10.1242/jcs.144386 PMID: 24849653

7. Buchberger A, Bukau B, Sommer T. Protein Quality Control in the Cytosol and the Endoplasmic Reticulum: Brothers in Arms. Molecular Cell. 2010; 40(2):238–52. https://doi.org/10.1016/j.molcel.2010.10.001 PMID: 20965419

8. Wilkinson KD. Ubiquitination and deubiquitination: targeting of proteins for degradation by the proteasome. Semin Cell Dev Biol. 2000; 11(3):141–8. Epub 2000/07/25. https://doi.org/10.1006/scdb.2000.0164 PMID: 10906270

9. Leznicki P, High S. SGTA antagonizes BAG6-mediated protein triage. Proceedings of the National Academy of Sciences. 2012; 109(47):19214–9. https://doi.org/10.1073/pnas.1209997109 PMID: 23129660

10. Swatek KN, Komander D. Ubiquitin modifications. Cell Research. 2016; 26(4):399–422. https://doi.org/10.1038/cr.2016.39 PMID: 27012465

11. Clague MJ, Coulson JM, Urbé S. Cellular functions of the DUBs. Journal of Cell Science. 2012; 125 (2):277. https://doi.org/10.1242/jcs.090985 PMID: 22357969

12. Mevissen TET, Komander D. Mechanisms of Deubiquitinase Specificity and Regulation. Annual Review of Biochemistry. 2017; 86(1):159–92. https://doi.org/10.1146/annurev-biochem-061516-044916 PMID: 28498721

13. Dayal S, Sparks A, Jacob J, Allende-Vega N, Lane DP, Saville MK. Suppression of the Deubiquitinating Enzyme USP5 Causes the Accumulation of Unanchored Polyubiquitin and the Activation of p53. Journal of Biological Chemistry. 2009; 284(8):5030–41. https://doi.org/10.1074/jbc.M805871200 PMID: 19098288

14. Hanpude P, Bhattacharya S, Dey AK, Maiti TK. Deubiquitinating enzymes in cellular signaling and disease regulation. IUBMB Life. 2015; 67(7):544–55. https://doi.org/10.1002/iub.1402 PMID: 26178252

15. Scaglione KM, Zavodszky E, Todi Sokol V, Patury S, Xu P, Rodríguez-Lebrón E, et al. Ube2w and Ataxin-3 Coordinately Regulate the Ubiquitin Ligase CHIP. Molecular Cell. 2011; 43(4):599–612. https://doi.org/10.1016/j.molcel.2011.05.036 PMID: 21855799

16. Zhang Z-R, Bonifacino JS, Hegde RS. Deubiquitinases sharpen substrate discrimination during membrane protein degradation from the ER. Cell. 2013; 154(3):609–22. https://doi.org/10.1016/j.cell.2013.06.038 PMID: 23890821

17. Crosas B, Hanna J, Kirkpatrick DS, Zhang DP, Tone Y, Hathaway Nathaniel A, et al. Ubiquitin Chains Are Remodeled at the Proteasome by Opposing Ubiquitin Ligase and Deubiquitinating Activities. Cell. 2006; 127(7):1401–13. https://doi.org/10.1016/j.cell.2006.09.051 PMID: 17190603

18. Fang NN, Zhu M, Rose A, Wu K-P, Mayor T. Deubiquitinase activity is required for the proteasomal degradation of misfolded cytosolic proteins upon heat-stress. Nature Communications. 2016; 7:12907. https://doi.org/10.1038/ncomms12907 PMID: 27698423

19. Chu Y, Dong X, Kang Y, Liu J, Zhang T, Yang C, et al. The Chaperone BAG6 Regulates Cellular Homeostasis between Autophagy and Apoptosis by Holding LC3B. iScience. 2020; 23(11):101708–. https://doi.org/10.1016/j.isci.2020.101708 PMID: 33241194

20. Xu Y, Cai M, Yang Y, Huang L, Ye Y. SGTA Recognizes a Noncanonical Ubiquitin-like Domain in the Bag6-Ubl4A-Trc35 Complex to Promote Endoplasmic Reticulum-Associated Degradation. Cell Reports. 2012; 2(6):1633–44. https://doi.org/10.1016/j.celrep.2012.11.010 PMID: 23246001

21. Liu Y, Soetandyo N, Lee J-G, Liu L, Xu Y, Clemons WM Jr., et al. USP13 antagonizes gp78 to maintain functionality of a chaperone in ER-associated degradation. eLife. 2014; 3:e01369–e. Epub 2014/01/14. https://doi.org/10.7554/eLife.01369 PMID: 24424410

22. Culver JA, Mariappan M. Deubiquitinases USP20/33 promote the biogenesis of tail-anchored membrane proteins. J Cell Biol. 2021; 220(5). Epub 2021/04/02. https://doi.org/10.1083/jcb.202004086 PMID: 33792613

23. Eisele F, Wolf DH. Degradation of misfolded protein in the cytoplasm is mediated by the ubiquitin ligase Ubr1. FEBS Letters. 2008; 582(30):4143–6. https://doi.org/10.1016/j.febslet.2008.11.015 PMID: 19041308

24. Heck JW, Cheung SK, Hampton RY. Cytoplasmic protein quality control degradation mediated by parallel actions of the E3 ubiquitin ligases Ubr1 and San1. Proceedings of the National Academy of Sciences of the United States of America. 2010; 107(3):1106–11. Epub 12/28. https://doi.org/10.1073/pnas.0910591107 PMID: 20080635.

25. Ravid T, Kreft SG, Hochstrasser M. Membrane and soluble substrates of the Doa10 ubiquitin ligase are degraded by distinct pathways. EMBO J. 2006; 25(3):533–43. Epub 2006/01/26. https://doi.org/10.1038/sj.emboj.7600946 PMID: 16437165

26. Kostova Z, Tsai YC, Weissman AM. Ubiquitin ligases, critical mediators of endoplasmic reticulum-associated degradation. Seminars in Cell & Developmental Biology. 2007; 18(6):770–9. https://doi.org/10.1016/j.semcdb.2007.09.002 PMID: 17950636

27. Burr ML, Cano F, Svobodova S, Boyle LH, Boname JM, Lehner PJ. HRD1 and UBE2J1 target misfolded MHC class I heavy chains for endoplasmic reticulum-associated degradation. Proceedings of the National Academy of Sciences. 2011; 108(5):2034. https://doi.org/10.1073/pnas.1016229108 PMID: 21245296

28. Fang S, Ferrone M, Yang C, Jensen JP, Tiwari S, Weissman AM. The tumor autocrine motility factor receptor, gp78, is a ubiquitin protein ligase implicated in degradation from the endoplasmic reticulum. Proceedings of the National Academy of Sciences. 2001; 98(25):14422. https://doi.org/10.1073/pnas.251401598 PMID: 11724934

29. Zattas D, Berk JM, Kreft SG, Hochstrasser M. A Conserved C-terminal Element in the Yeast Doa10 and Human MARCH6 Ubiquitin Ligases Required for Selective Substrate Degradation*. Journal of Biological Chemistry. 2016; 291(23):12105–18. https://doi.org/10.1074/jbc.M116.726877 PMID: 27068744

30. Stefanovic-Barrett S, Dickson AS, Burr SP, Williamson JC, Lobb IT, van den Boomen DJ, et al. MARCH6 and TRC8 facilitate the quality control of cytosolic and tail-anchored proteins. EMBO reports. 2018; 19(5):e45603. Epub 03/08. https://doi.org/10.15252/embr.201745603 PMID: 29519897

31. Rodrigo-Brenni Monica C, Gutierrez E, Hegde Ramanujan S. Cytosolic Quality Control of Mislocalized Proteins Requires RNF126 Recruitment to Bag6. Molecular Cell. 2014; 55(2):227–37. https://doi.org/10.1016/j.molcel.2014.05.025 PMID: 24981174

32. Wunderley L, Leznicki P, Payapilly A, High S. SGTA regulates the cytosolic quality control of hydrophobic substrates. Journal of cell science. 2014; 127(Pt 21):4728–39. Epub 2014/09/01. https://doi.org/10.1242/jcs.155648 PMID: 25179605.

33. Waheed AA, MacDonald S, Khan M, Mounts M, Swiderski M, Xu Y, et al. The Vpu-interacting Protein SGTA Regulates Expression of a Non-glycosylated Tetherin Species. Scientific reports. 2016; 6:24934–. https://doi.org/10.1038/srep24934 PMID: 27103333

34. Yamamoto K, Hayashishita M, Minami S, Suzuki K, Hagiwara T, Noguchi A, et al. Elimination of a signal sequence-uncleaved form of defective HLA protein through BAG6. Scientific reports. 2017; 7(1):14545–. https://doi.org/10.1038/s41598-017-14975-9 PMID: 29109525

35. Suzuki R, Kawahara H. UBQLN4 recognizes mislocalized transmembrane domain proteins and targets these to proteasomal degradation. EMBO reports. 2016; 17(6):842. https://doi.org/10.15252/embr.201541402 PMID: 27113755

36. Minami R, Hayakawa A, Kagawa H, Yanagi Y, Yokosawa H, Kawahara H. BAG-6 is essential for selective elimination of defective proteasomal substrates. The Journal of Cell Biology. 2010; 190(4):637. https://doi.org/10.1083/jcb.200908092 PMID: 20713601

37. Kuwabara N, Minami R, Yokota N, Matsumoto H, Senda T, Kawahara H, et al. Structure of a BAG6 (Bcl-2-associated Athanogene 6)-Ubl4a (Ubiquitin-like Protein 4a) Complex Reveals a Novel Binding Interface That Functions in Tail-anchored Protein Biogenesis. Journal of Biological Chemistry. 2015; 290(15):9387–98. https://doi.org/10.1074/jbc.M114.631804 PMID: 25713138

38. Darby JF, Krysztofinska EM, Simpson PJ, Simon AC, Leznicki P, Sriskandarajah N, et al. Solution structure of the SGTA dimerisation domain and investigation of its interactions with the ubiquitin-like domains of BAG6 and UBL4A. PloS one. 2014; 9(11):e113281–e. https://doi.org/10.1371/journal.pone.0113281 PMID: 25415308

39. Chartron Justin W, VanderVelde David G, Clemons William M. Structures of the Sgt2/SGTA Dimerization Domain with the Get5/UBL4A UBL Domain Reveal an Interaction that Forms a Conserved Dynamic Interface. Cell Reports. 2012; 2(6):1620–32. https://doi.org/10.1016/j.celrep.2012.10.010 PMID: 23142665

40. Dutta S, Tan Y-J. Structural and Functional Characterization of Human SGT and Its Interaction with Vpu of the Human Immunodeficiency Virus Type 1. Biochemistry. 2008; 47(38):10123–31. https://doi.org/10.1021/bi800758a PMID: 18759457

41. Thapaliya A, Nyathi Y, Martínez-Lumbreras S, Krysztofinska EM, Evans NJ, Terry IL, et al. SGTA interacts with the proteasomal ubiquitin receptor Rpn13 via a carboxylate clamp mechanism. Scientific Reports. 2016; 6:36622. https://doi.org/10.1038/srep36622 https://www.nature.com/articles/srep36622#supplementary-information. PMID: 27827410

42. Liou S-T, Wang C. Small glutamine-rich tetratricopeptide repeat-containing protein is composed of three structural units with distinct functions. Archives of Biochemistry and Biophysics. 2005; 435(2):253–63. https://doi.org/10.1016/j.abb.2004.12.020 PMID: 15708368

43. Leznicki P, Korac-Prlic J, Kliza K, Husnjak K, Nyathi Y, Dikic I, et al. Binding of SGTA to Rpn13 selectively modulates protein quality control. Journal of Cell Science. 2015; 128(17):3187. https://doi.org/10.1242/jcs.165209 PMID: 26169395

44. Hu X, Wang L, Wang Y, Ji J, Li J, Wang Z, et al. RNF126-Mediated Reubiquitination Is Required for Proteasomal Degradation of p97-Extracted Membrane Proteins. Mol Cell. 2020; 79(2):320–31.e9. Epub 2020/07/10. https://doi.org/10.1016/j.molcel.2020.06.023 PMID: 32645369

45. Dantuma NP, Lindsten K, Glas R, Jellne M, Masucci MG. Short-lived green fluorescent proteins for quantifying ubiquitin/proteasome-dependent proteolysis in living cells. Nat Biotechnol. 2000; 18(5):538–43. Epub 2000/05/10. https://doi.org/10.1038/75406 PMID: 10802622

46. Martínez-Lumbreras S, Krysztofinska EM, Thapaliya A, Spilotros A, Matak-Vinkovic D, Salvadori E, et al. Structural complexity of the co-chaperone SGTA: a conserved C-terminal region is implicated in dimerization and substrate quality control. BMC Biology. 2018; 16(1):76. https://doi.org/10.1186/s12915-018-0542-3 PMID: 29996828

47. Payapilly A, High S. BAG6 regulates the quality control of a polytopic ERAD substrate. Journal of Cell Science. 2014; 127(13):2898. https://doi.org/10.1242/jcs.145565 PMID: 24806960

48. Walczak CP, Ravindran MS, Inoue T, Tsai B. A cytosolic chaperone complexes with dynamic membrane J-proteins and mobilizes a nonenveloped virus out of the endoplasmic reticulum. PLoS Pathog [Internet]. 2014 2014/03//; 10(3):[e1004007 p.]. https://doi.org/10.1371/journal.ppat.1004007 PMID: 24675744

49. Kim E, Park S, Lee JH, Mun JY, Choi WH, Yun Y, et al. Dual Function of USP14 Deubiquitinase in Cellular Proteasomal Activity and Autophagic Flux. Cell Reports. 2018; 24(3):732–43. https://doi.org/10.1016/j.celrep.2018.06.058 PMID: 30021169

50. Kim DI, Jensen SC, Noble KA, Kc B, Roux KH, Motamedchaboki K, et al. An improved smaller biotin ligase for BioID proximity labeling. Mol Biol Cell. 2016; 27(8):1188–96. Epub 2016/02/24. https://doi.org/10.1091/mbc.E15-12-0844 PMID: 26912792

51. Bromfield E, Aitken RJ, Nixon B. Novel characterization of the HSPA2-stabilizing protein BAG6 in human spermatozoa. Molecular Human Reproduction. 2015; 21(10):755–69. https://doi.org/10.1093/molehr/gav041 PMID: 26153132

52. Urbé S, Liu H, Hayes SD, Heride C, Rigden DJ, Clague MJ. Systematic survey of deubiquitinase localization identifies USP21 as a regulator of centrosome- and microtubule-associated functions. Mol Biol Cell. 2012; 23(6):1095–103. Epub 2012/02/03. https://doi.org/10.1091/mbc.E11-08-0668 PMID: 22298430

53. Borodovsky A, Kessler BM, Casagrande R, Overkleeft HS, Wilkinson KD, Ploegh HL. A novel active site-directed probe specific for deubiquitylating enzymes reveals proteasome association of USP14. EMBO J. 2001; 20(18):5187–96. Epub 2001/09/22. https://doi.org/10.1093/emboj/20.18.5187 PMID: 11566882

54. Muniyappan S, Lee B-H. Chapter Eleven—In vitro analysis of proteasome-associated USP14 activity for substrate degradation and deubiquitylation. In: Hochstrasser M, editor. Methods in Enzymology. 619: Academic Press; 2019. p. 249–68.

55. Lee BH, Lu Y, Prado MA, Shi Y, Tian G, Sun S, et al. USP14 deubiquitinates proteasome-bound substrates that are ubiquitinated at multiple sites. Nature. 2016; 532(7599):398–401. Epub 2016/04/14. https://doi.org/10.1038/nature17433 PMID: 27074503

56. Ray-Sinha A, Cross BC, Mironov A, Wiertz E, High S. Endoplasmic reticulum-associated degradation of a degron-containing polytopic membrane protein. Mol Membr Biol. 2009; 26(8):448–64. Epub 2009/11/03. https://doi.org/10.3109/09687680903333839 PMID: 19878048

57. Lilienbaum A. Relationship between the proteasomal system and autophagy. Int J Biochem Mol Biol. 2013; 4(1):1–26. PMID: 23638318.

58. Zhang Y-H, Zhou C-J, Zhou Z-R, Song A-X, Hu H-Y. Domain analysis reveals that a deubiquitinating enzyme USP13 performs non-activating catalysis for Lys63-linked polyubiquitin. PloS one. 2011; 6(12): e29362–e. Epub 2011/12/28. https://doi.org/10.1371/journal.pone.0029362 PMID: 22216260

59. Scott D, Layfield R, Oldham NJ. Structural insights into interactions between ubiquitin specific protease 5 and its polyubiquitin substrates by mass spectrometry and ion mobility spectrometry. Protein Science. 2015; 24(8):1257–63. https://doi.org/10.1002/pro.2692 PMID: 25970461

60. Liu Q, Wu Y, Qin Y, Hu J, Xie W, Qin FX-F, et al. Broad and diverse mechanisms used by deubiquitinase family members in regulating the type I interferon signaling pathway during antiviral responses. Science Advances. 2018; 4(5):eaar2824. https://doi.org/10.1126/sciadv.aar2824 PMID: 29732405

61. Tamar Hadari S, Jessie V. B. Warmst Irwin Rose A., Hershko A. A Ubiquitin C-terminal Isopeptidase That Acts on Polyubiquitin Chains. ROLE IN PROTEIN DEGRADATION*. Journal of Biological Chemistry. 1992; 267(2):719–27. PMID: 1309773

62. Wilkinson KD, Tashayev VL, O'Connor LB, Larsen CN, Kasperek E, Pickart CM. Metabolism of the polyubiquitin degradation signal: structure, mechanism, and role of isopeptidase T. Biochemistry. 1995; 34(44):14535–46. https://doi.org/10.1021/bi00044a032 PMID: 7578059

63. Raasi S, Varadan R, Fushman D, Pickart CM. Diverse polyubiquitin interaction properties of ubiquitin-associated domains. Nature Structural & Molecular Biology. 2005; 12(8):708–14. https://doi.org/10.1038/nsmb962 PMID: 16007098

64. Ning F, Xin H, Liu J, Lv C, Xu X, Wang M, et al. Structure and function of USP5: Insight into physiological and pathophysiological roles. Pharmacol Res. 2020; 157:104557. Epub 2019/11/23. https://doi.org/10.1016/j.phrs.2019.104557 PMID: 31756387

65. Li X-Y, Wu H-Y, Mao X-F, Jiang L-X, Wang Y-X. USP5 promotes tumorigenesis and progression of pancreatic cancer by stabilizing FoxM1 protein. Biochemical and Biophysical Research Communications. 2017; 492(1):48–54. https://doi.org/10.1016/j.bbrc.2017.08.040 PMID: 28807830

66. García-Caballero A, Gadotti Vinicius M, Stemkowski P, Weiss N, Souza Ivana A, Hodgkinson V, et al. The Deubiquitinating Enzyme USP5 Modulates Neuropathic and Inflammatory Pain by Enhancing Cav3.2 Channel Activity. Neuron. 2014; 83(5):1144–58. https://doi.org/10.1016/j.neuron.2014.07.036 PMID: 25189210

67. Meng J, Ai X, Lei Y, Zhong W, Qian B, Qiao K, et al. USP5 promotes epithelial-mesenchymal transition by stabilizing SLUG in hepatocellular carcinoma. Theranostics. 2019; 9(2):573–87. https://doi.org/10.7150/thno.27654 PMID: 30809294

68. Li G, Yang T, Chen Y, Bao J, Wu D, Hu X, et al. USP5 Sustains the Proliferation of Glioblastoma Through Stabilization of CyclinD1. Front Pharmacol. 2021; 12:720307–. https://doi.org/10.3389/fphar.2021.720307 PMID: 34483932

69. Wang S, Juan J, Zhang Z, Du Y, Xu Y, Tong J, et al. Inhibition of the deubiquitinase USP5 leads to c-Maf protein degradation and myeloma cell apoptosis. Cell Death Dis. 2017; 8(9):e3058–e. https://doi.org/10.1038/cddis.2017.450 PMID: 28933784

70. Xie X, Matsumoto S, Endo A, Fukushima T, Kawahara H, Saeki Y, et al. Deubiquitylases USP5 and USP13 are recruited to and regulate heat-induced stress granules through their deubiquitylating activities. Journal of Cell Science. 2018; 131(8):jcs210856. https://doi.org/10.1242/jcs.210856 PMID: 29567855

71. Yesbolatova A, Saito Y, Kitamoto N, Makino-Itou H, Ajima R, Nakano R, et al. The auxin-inducible degron 2 technology provides sharp degradation control in yeast, mammalian cells, and mice. Nature communications. 2020; 11(1):5701–. https://doi.org/10.1038/s41467-020-19532-z PMID: 33177522

72. Ganji R, Mukkavalli S, Somanji F, Raman M. The VCP-UBXN1 complex mediates triage of ubiquitylated cytosolic proteins bound to the BAG6 complex. Molecular and cellular biology. 2018; 38(13):e00154–18. https://doi.org/10.1128/MCB.00154-18 PMID: 29685906

73. Song A-X, Yang H, Gao Y-G, Zhou C-J, Zhang Y-H, Hu H-Y. A Ubiquitin Shuttle DC-UbP/UBTD2 Reconciles Protein Ubiquitination and Deubiquitination via Linking UbE1 and USP5 Enzymes. PLOS ONE. 2014; 9(9):e107509. https://doi.org/10.1371/journal.pone.0107509 PMID: 25207809